NASA TECHNICAL NOTE

NASA TN D-3705

NASA TN D-3705

PHOTOGRAPHIC STUDY OF MERCURY DROPLET PARAMETERS INCLUDING EFFECTS OF GRAVITY

by Jonas I. Sturas, Clifford C. Crabs, and Sol H. Gorland

Lewis Research Center
Cleveland, Ohio

NATIONAL AERONAUTICS AND SPACE ADMINISTRATION • WASHINGTON, D. C. • NOVEMBER 1966

NASA TN D-3705

PHOTOGRAPHIC STUDY OF MERCURY DROPLET PARAMETERS INCLUDING EFFECTS OF GRAVITY

By Jonas I. Sturas, Clifford C. Crabs, and Sol H. Gorland

Lewis Research Center
Cleveland, Ohio

NATIONAL AERONAUTICS AND SPACE ADMINISTRATION

For sale by the Clearinghouse for Federal Scientific and Technical Information
Springfield, Virginia 22151 – Price $2.00

PHOTOGRAPHIC STUDY OF MERCURY DROPLET PARAMETERS INCLUDING EFFECTS OF GRAVITY

by Jonas I. Sturas, Clifford C. Crabs, and Sol.H. Gorland

Lewis Research Center

SUMMARY

A photographic study was conducted of mercury droplet behavior in gravity environments of 0, 1, $1\frac{1}{2}$, and 2 g's primarily to obtain a simple, and at the same time reliable, method for determining various geometric parameters and shape factors of a sessile mercury droplet in a glass tube. Specific emphasis was placed on those characteristic parameters that would be useful in flow-regime and heat-transfer analyses associated with dropwise condensation of mercury vapor.

It is shown that the contact angle of a given size sessile droplet with a solid surface is a function of two dimensionless parameters, size factor and shape factor, which are both dependent on gravity level and are obtained from droplet measurements. Therefore, the method presented herein for determining the contact angle of a sessile droplet is general and applicable to various gravity environments. It is shown that the contact angles calculated from measured droplet dimensions are just as accurate as those obtained by measuring the angles directly from enlarged photographs of a droplet.

Empirical equations were developed for expressing the geometric droplet parameters investigated in various environments of gravity. The contact angle increased with an increase in gravity level by a greater amount for large droplets than for small droplets. In a positive gravity environment, the mean contact angle increases with mean diameter of the droplet and approaches a maximum equilibrium value at some fixed droplet size. The contact angle formed by a droplet and a glass tube in a zero-gravity environment is independent of droplet size and approaches a constant value of 139° obtained by using a root-mean-square method. Tests run in a 1-g environment showed that the thermal equilibrium between mercury and glass (which resulted in a constant contact angle) was obtained within 60 to 80 minutes.

INTRODUCTION

The analysis of boiling and condensing heat-transfer characteristics of nonwetting fluids depends on knowledge of geometric parameters of liquid droplets in contact with the solid surface, such as contact areas with solids, surface areas exposed to the vapor phase, and droplet volumes that are the functions of contact angle. Analyses of nonwetting condensation are reported in references 1 and 2; they are based on contact angle as an independent variable but have not considered the effects of droplet size and gravity environment on contact angle, and, hence, on droplet shape.

The effect of droplet size on its contact angle (and, therefore, droplet shape) has been reported by Bashforth and Adams in reference 3 and by Mack in reference 4. However, the effect of gravity environment on droplet characteristics has previously not been included. Therefore, as part of an overall study of mercury boiling and condensing problems associated with space power systems utilizing mercury vapor as the working fluid, an investigation was conducted at the Lewis Research Center to determine the effect of gravity environments on contact angle and geometric parameters of mercury droplets.

The primary objective of this study was to determine experimentally the geometric characteristics of sessile droplets of various sizes in a glass tube from photographic data obtained in gravity environments of 0, 1, $1\frac{1}{2}$, and 2 g's. The droplet geometric characteristics include contact angle, contact diameter, contact area with tube wall, and surface area exposed to the vapor phase. These data were obtained experimentally in each gravity environment under study.

The secondary objective was to obtain empirical expressions defining the geometric characteristics of droplets in terms of a mean droplet diameter. In addition to these data, the effect of time-in-position on contact angle of a sessile mercury droplet with glass and the dynamic contact angles of various size droplets sliding in an inclined glass tube in a 1-g environment were also obtained.

APPARATUS AND PROCEDURE

Three types of apparatus were used for the droplet tests performed. The test conditions were (1) steady-state 1-g environment, (2) steady-state zero-gravity and multigravity environments, and (3) dynamic 1-g environment.

Photographic Techniques

Individually encapsulated mercury droplets were photographed in various gravity environments. Geometric droplet parameter data were obtained by analyzing enlarged drop-

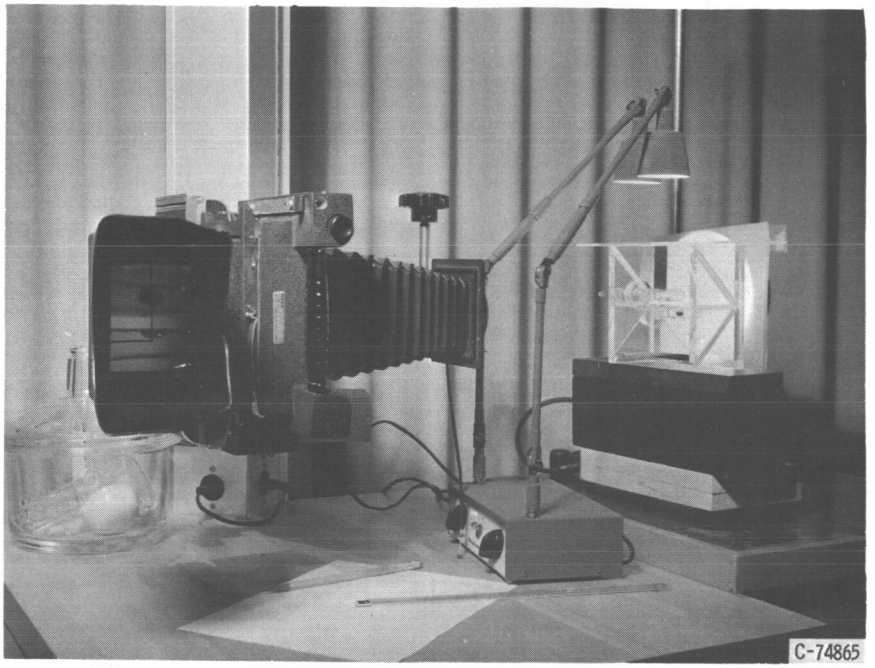

Figure 1. - Experimental setup for 1-g environment.

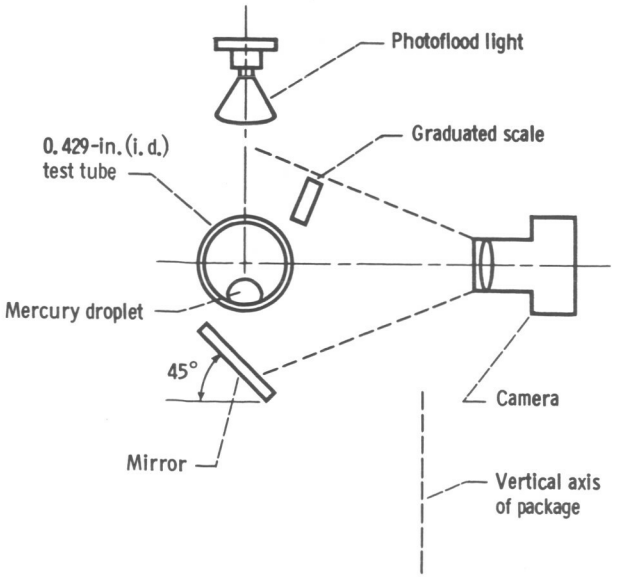

Figure 2. - Schematic diagram of relation of camera, test tube, mirror and light for zero-gravity and multi-gravity environments.

let photographs. The setup used for photographing a sessile mercury droplet in a glass tube (figs. 1 and 2) consisted essentially of a cylindrical glass capsule 0.429 inch in inside diameter by 1.625 inches long, welded to a ground joint 0.394 inch in inside diameter by 1.181 inches long. The sealed capsule (fig. 3) contained a single mercury droplet of a known weight.

The capsule was mounted horizontally in a transparent frame in a position that allowed the camera to be rotated to any angular position around the capsule, as illustrated in figure 2. Thus, a side view, a top view, and a bottom view of each droplet at a given interval of time-in-position could be photographed. In addition, the contact area of a sessile droplet with the capsule wall was simultaneously photographed while taking the sideview picture by using the mirror mounted below the capsule into the frame at an angle of 45^{o}. A

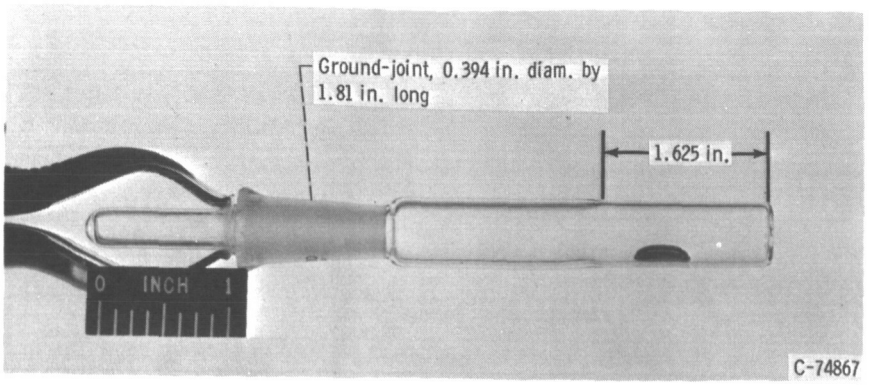

Figure 3. - Enclosed mercury droplet in glass tube for 1-g (ground) tests.

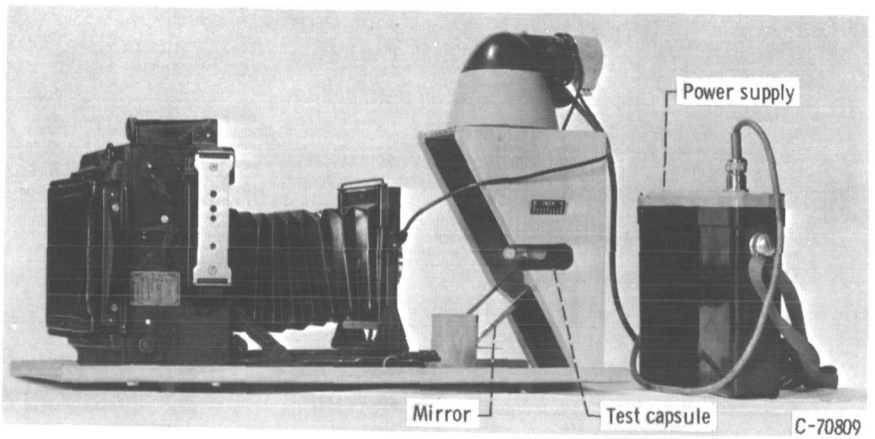

Figure 4. - Experimental airplane setup for 0-, $1\frac{1}{2}$-, and 2-g environments.

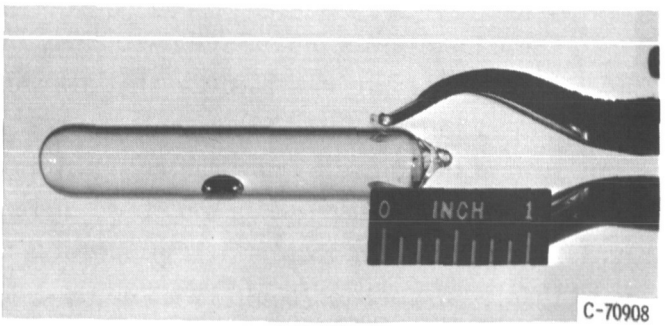

Figure 5. - Encapsulated mercury droplet in glass tube for tests at 0, $1\frac{1}{2}$, and 2 g's.

camera with a 23^{o} field-of-view lens, was located opposite the test section of a specimen to be photographed. For a parametric analysis, the pictures were enlarged 5 to 100 times, depending on which scale gave the largest magnified high-contrast image of the droplet profile.

The airplane test setup used to photograph individual mercury droplets in 0-, $1\frac{1}{2}$-, and 2-g environments (fig. 4) consisted essentially of a cylindrical glass tube 0.429 inch in inside diameter and 2.500 inches long (fig. 5). Droplets of known weight were encapsulated more

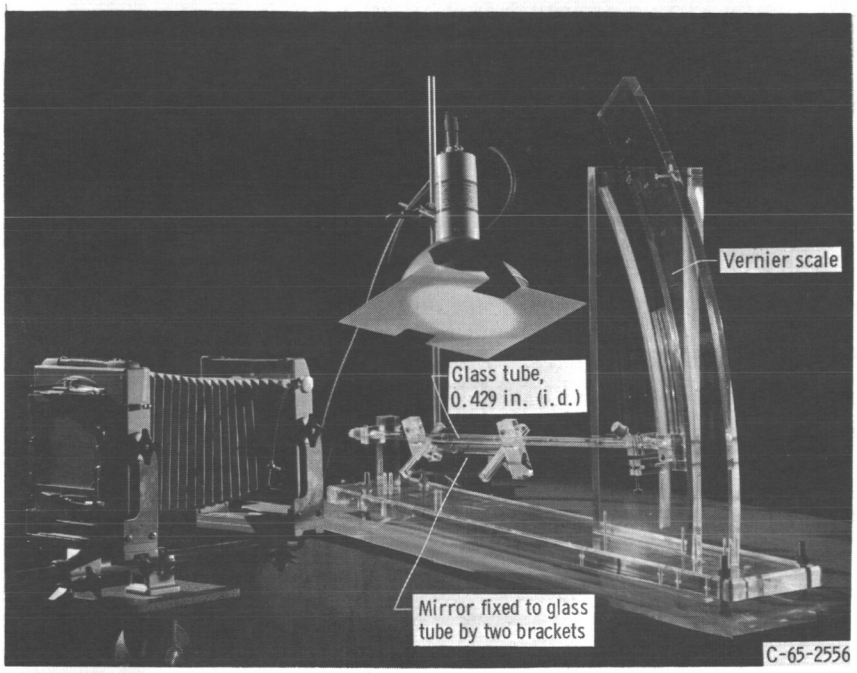

(a) Overall view.

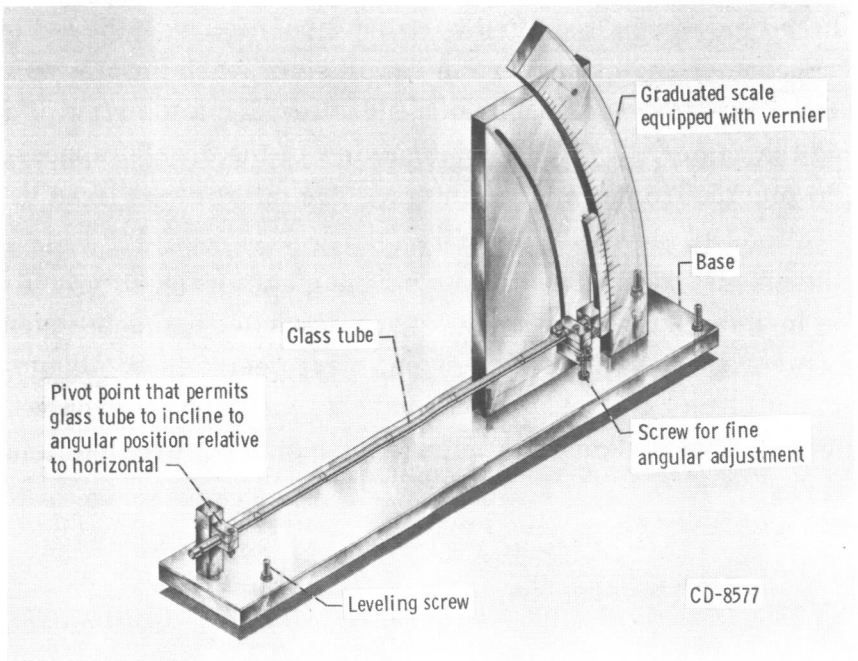

(b) Detail.

Figure 6. - Setup for photographing mercury droplets in motion under the influence of gravity in an inclined glass tube 0.429 inch in diameter.

than 2 hours before the test in order to reach thermal equilibrium. The glass capsule was horizontally mounted in a frame a few minutes prior to the test.

In order to obtain a photograph of the side view and the bottom view of a droplet simultaneously, a mirror was mounted into the frame below the test capsule at an angle of 45^{o}, as in the 1-g tests (fig. 2).

A camera with a 25^{o} field-of-view lens was rigidly attached to a test fixture 4 inches from the capsule. Droplet photographs obtained in various gravity fields were enlarged 5 to 10 times and used for a parametric analysis.

The test fixture for photographing moving mercury droplets in a glass tube (fig. 6) consisted of a cylindrical glass tube 0.429 inch in diameter and 31 inches long. The left end of the tube was fixed to a pivot point mounted to the base of the fixture. The pivot point permitted change of the inclination of the tube from 0^{o} to 35^{o}. A vernier protractor fixed to the right end of the tube was used to measure the inclination angle. Thus, for a given mercury droplet, the tube inclination for incipient motion could be determined. The average velocity of a sliding mercury droplet was determined by recording the droplet translation time between the two length marks along the tube with a stop watch having an accuracy of 0.10 second.

Fifteen mercury droplets of known weight were analyzed in the dynamic tests. A single droplet was placed into a glass tube, as shown in figure 6(a) and both the base of the test fixture and the tube were alined in a horizontal position with the aid of a spirit level. In order to obtain contact angles at thermal equilibrium, each droplet was allowed to stay in position for 60 minutes. Photographs of a side view and a top view of a droplet were taken by rotating the camera, while the bottom view of the droplet appeared simultaneously with the sideview picture from a mirror image. The mirror was fixed to the glass tube below the test section, as shown in figure 6(a).

Motion of the droplet was induced by an incremental increase in inclination of the glass tube. The incipient movement angle, dynamic angle, and subsequent drop velocity as the droplets traversed the length of the tube, were determined. Photographs were taken at the moment of incipient movement and at a fixed tube location while the droplets were moving along the tube. For a parametric analysis, the droplet pictures were enlarged 5 to 10 times.

Measurement of Time Required for Thermal Equilibrium

In order to determine the time required for thermal equilibrium, two sets of mercury droplets were analyzed. First, 10 droplets ranging in weight from 14.40×10^{-4} to 694.40×10^{-4} ounce were allowed to stay in position in a horizontally alined glass capsule for time intervals of 1 and 24 hours. Initial and terminal time pictures of side view, top

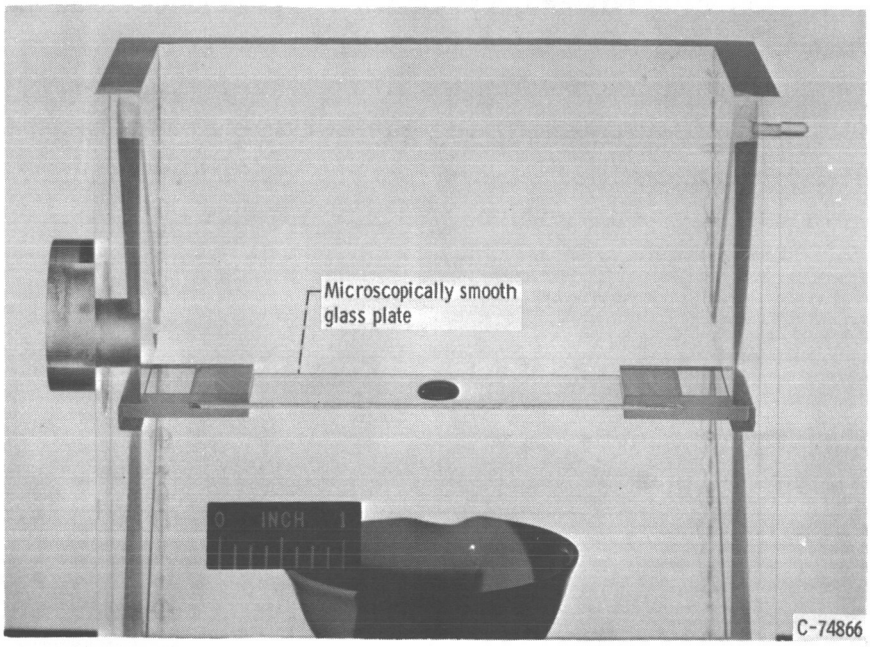

Figure 7. - Perspective view of sessile mercury droplet on microscopically smooth glass plate fixed in transparent frame.

view, and bottom view were taken of each individual droplet. Second, eight droplets ranging in weight from 11.80×10^{-4} to 731.40×10^{-4} ounce were photographed in a horizontally alined capsule, and then each droplet was placed on a horizontally alined, microscopically smooth glass plate, such as that shown in figure 7, and pictures of the side view (which included a mirror image of the contact area with glass) were taken at time-in-position intervals ranging from 1 to 155 minutes. In order to prevent oxidation of the mercury droplet surface due to direct contact with atmospheric air during the waiting period, each droplet on a glass plate had been covered with a small glass cup purged with nitrogen gas.

Cleanliness of Glass Surfaces

For each droplet tested, the glass capsule, or glass plate, and also a glass dropper with which a mercury droplet was picked up and inserted into a test capsule were cleaned by first treating the surfaces with dilute nitric acid (HNO_3), followed by washing with a large quantity of soapy water, flushing with distilled water, and finally steaming and heating to 930° F in air for 2 hours. After these glass capsules, glass plates, or a glass dropper, were cooled slowly, they exhibited zero solid-water-air contact angles, indicating the degree of cleanliness. The prepared glass capsules containing mercury droplets, cleaned glass plates, and glass droppers were stored in a clean glass container that

was purged with nitrogen gas. During the test period, the glass container with the test specimens was kept hermetically sealed

The fluid used in this analysis was triple distilled mercury. During the experimental investigation, the mercury was essentially at ambient pressure and temperature. The physical properties of triple distilled mercury, as reported by Wheatherford (ref. 5), are as follows:

Atomic weight	200.61
Boiling point, ^{o}F	674.00
Density (at 70^{o} F), lb/cu ft	838.00
Melting point, ^{o}F	-37.97
Specific heat (at 70^{o} F), Btu/(lb)(^{o}F)	0.3350
Surface tension (at 70^{o} F), lb/ft	0.03188
Viscosity (at 70^{o} F), lb/(ft)(hr)	3.71

METHOD OF ANALYSIS

The geometric characteristics are basically dependent functions of the droplet contact angle. The contact angles were obtained by both direct measurements from enlarged droplet photographs and also by calculation from droplet dimension. The following description deals with the relations developed to describe sessile and dynamic droplet contact angles, droplet contact area with a solid surface, droplet surface area exposed to the vapor phase, and droplet volume.

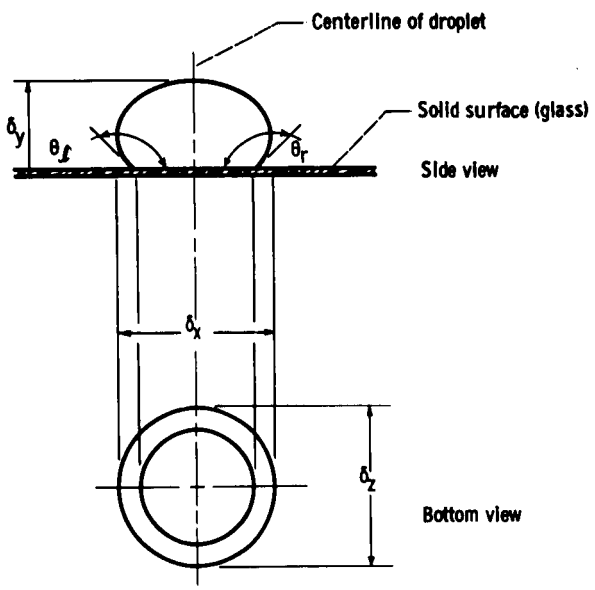

Figure 8. - Method used to locate droplet contact with solid surface.

Measured Contact Angle

The mean contact angle of a sessile mercury droplet on a horizontal solid surface in 0-, 1-, $1\frac{1}{2}$-, and 2-g environments was determined from the contact angles measured at two points as shown in figure 8; θ_ℓ is the contact angle on the left side and θ_r is the contact angle on the right side of the droplet. Thus,

$$\theta_{s,m} = \frac{\theta_\ell + \theta_r}{2} \qquad (1)$$

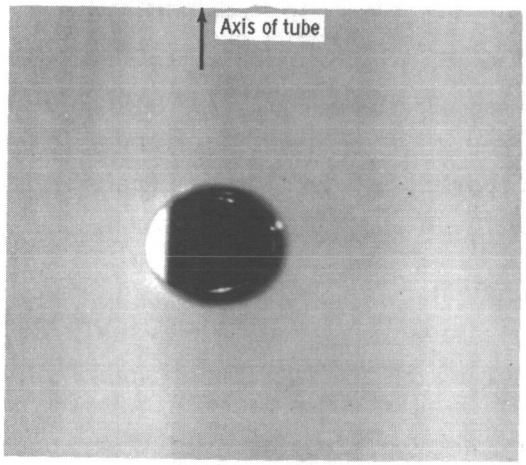

(a) Mean droplet diameter, 0.0575 inch.

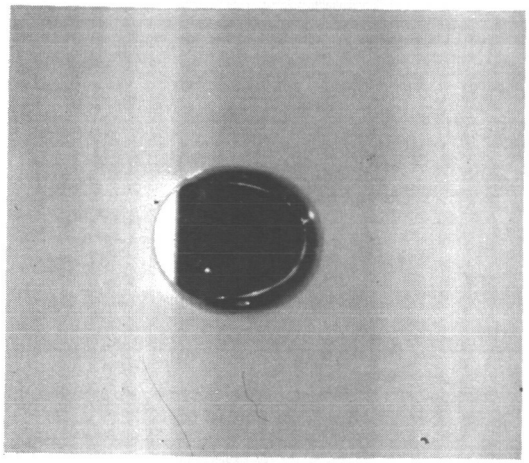

(b) Mean droplet diameter 0.0713 inch.

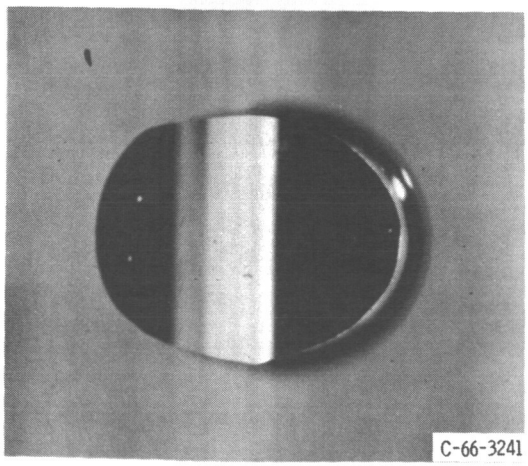

(c) Mean droplet diameter, 0.1500 inch.

Figure 9. - Variation of mercury droplet contact area with mean diameter. Undisturbed droplet inside of glass tube (inside diameter, 0.429 in.) in 1-g environment. X10.

In order to measure droplet contact angle directly, a point of droplet contact with the solid surface was established from the bottom view of a droplet, as shown in figure 9. Once the point of droplet contact was established, the tangent to the curved droplet surface from the point of contact was drawn, and the angle was measured with the aid of a protractor equipped with a calibrated vernier, and 5× magnifying glass. All the measurements were made from enlarged pictures.

In the dynamic tests, the advancing and receding points of contact of a droplet with the solid were established by the use of the droplet side view in conjunction with the bottom view taken from the mirror image, as illustrated in figure 8. The advancing θ_A and receding θ_R contact angles of a moving droplet were directly measured from the enlarged photographs. The distortion angle of a droplet moving at a given average velocity was calculated from the equation

$$\Delta\theta = \frac{\theta_A - \theta_R}{2} \qquad (2)$$

The mean dynamic contact angle of a droplet was calculated from the equation

$$\theta_d = \frac{\theta_A + \theta_R}{2} \qquad (3)$$

Calculated Contact Angle

In addition to measuring the contact angle directly, it was calculated from the dimensions of the droplet by the method of Bashforth and Adams (ref. 3). The droplet contact angle was related to the droplet size factor $2\delta_y/\delta$ and droplet shape factor $\delta/2b$. Droplet radius of

curvature b at its apex, which defines the shape factor of a given droplet, was calculated from Rayleigh's equation (ref. 6)

$$b = r + \frac{r^3}{3c^2} - \frac{2r^5}{(3c^2)^2}(3 \ln 2 - 2) + \frac{r^7}{(3c^2)^3}(78 \ln 72 - 53) \tag{4}$$

where $r = \delta/2$ and c^2 is the Laplacian capillary constant.

In the droplet size range under investigation, the values of r/c are very small, and the last two terms in equation (4) add little to the accuracy of b. Therefore, the simplified equation results in

$$b = r + \frac{1}{3}\frac{r^3}{c^2} = \frac{1}{24}\left(12\delta + \frac{\delta^3}{c^2}\right) \tag{5}$$

where δ is the mean diameter of the droplet determined by

$$\delta = \frac{\delta_x + \delta_z}{2}$$

as shown in figure 8.

The value of the Laplacian capillary constant c^2 of each droplet analyzed was calculated from the following equation

$$c^2 = \frac{\delta^2}{4}\left(\frac{0.05200}{f} - 0.12268 + 0.04810\, f\right) \tag{6}$$

derived empirically by Dorsey (ref. 7), where the deviation of the droplet from actual spherical shape is

$$f = \frac{2(X_{135} - K_{135})}{\delta} - 0.41421 \tag{7}$$

The dimensions in equations (6) and (7), indicated in figure 10, are taken from reference 7. As indicated in figure 10, E is any point on the 135° tangent below the point B. From the geometry of a droplet, the value of $(X_{135} - K_{135})$ is equal to the distance CB (= DE - DB). If a droplet were spherical with radius $r = \delta/2$, CB would be equal to $(\sqrt{2} - 1)\frac{\delta}{2} = 0.41421\left(\frac{\delta}{2}\right)$.

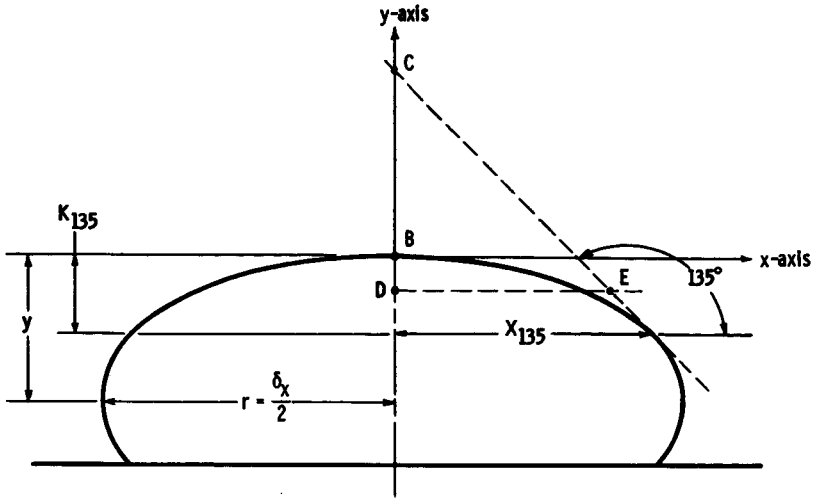

Figure 10. - Droplet dimensions. (B, C, D, and E are intersections.)

Equation (7) contains only linear quantities that were readily obtained from a photograph of the profile of the droplet surface. An error of 0.001 in f will produce an error of 0.80 percent in c^2. When the values of b and c^2 have been determined, the geometry droplet parameters β, $(\delta/2b)$, y/b, and $2\delta_y/\delta$ were calculated for each droplet analyzed. In this analysis, droplet dimensions have been selected (other than those given in ref. 3) that may be measured precisely from enlarged droplet photographs, or that may be readily calculated from other experimental data. For each value of $\delta/2b$ and y/b calculated, the contact angle $\theta_{s,c}$ was obtained by the numerical interpolation of the original tables of Bashforth and Adams. The values of $\theta_{s,c}$ recorded in tables I to IV are correct to the nearest 0.1°, relative to the original tables given in reference 3.

Droplet Geometric Parameters

The contact area of a sessile droplet with a wall of a glass tube was measured with a planimeter from enlarged droplet pictures such as those shown in figure 9. This value was multiplied by a correction factor to account for the tube wall curvature,

$$A_c = A_m \frac{L_t}{L_a} \tag{8}$$

where L_a is the apparent major axis of the ellipse of the droplet in contact with the tube wall, L_t is the true length of the major axis of the ellipse of the droplet in contact with tube wall, and is $\pi/180\,(\gamma r)$. This expression was derived from the geometry of a droplet in contact with the tube wall shown in figure 11.

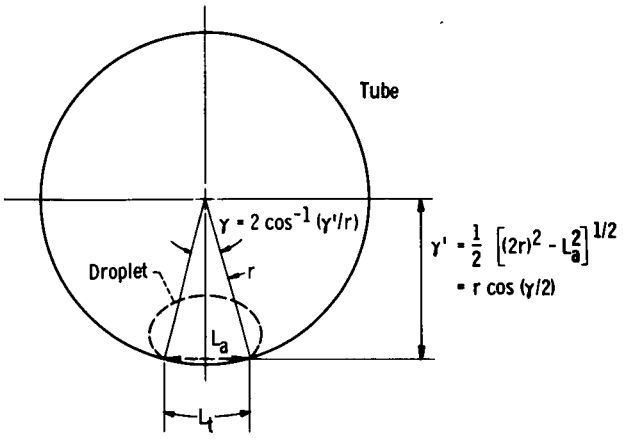

Figure 11. - Geometry of droplet in contact with tube wall.

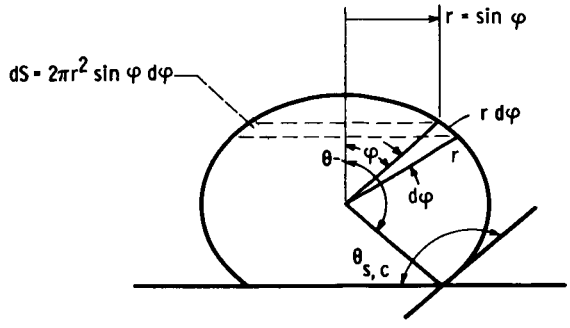

Figure 12. - Integration method for calculating free-surface area of droplet.

The ratio of the contact area of a droplet on the curve tube wall to that on a flat plate can be defined by the contact area shape correction factor

$$F = \frac{A_c}{A_{cir}} \tag{9}$$

where

$$A_{cir} = \frac{\pi}{4} d^2$$

and d is the minor axis of the droplet contact ellipse. The values of F are dependent on the gravity environmental conditions.

In the droplet size range investigated (0.0116 to 0.2250 in. in diam), the surface area of a sessile droplet exposed to the vapor phase was estimated by two different methods. The first method was used mainly for small droplets, $\leq$0.065 inch, and was related to the contact angle of a given size sessile droplet with the shape of a spherical segment, as shown in figure 12. The surface area is obtained from the following integration:

$$\left.\begin{aligned} S &= \int ds \\ &= 2\pi r^2 \int_{\varphi=0}^{\varphi=\theta_{s,c}} \sin\varphi\, d\varphi \\ &= 2\pi r^2(1 - \cos\theta_s) \\ &= \frac{\pi}{2}\delta^2(1 - \cos\theta_s) \end{aligned}\right\} \tag{10}$$

Equation (10) is accurate for small droplets that are negligibly flattened by gravity and for all droplet sizes in a zero-gravity environment. Since larger droplets were significantly flattened by gravity, resulting in ellipsoidal shapes, a second method, involving a

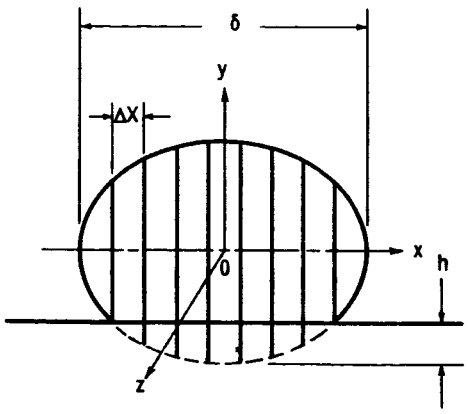

Figure 13. - Numerical approximation method for calculating free-surface area of droplet.

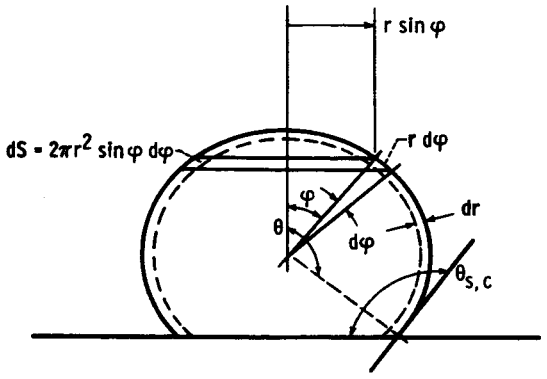

Figure 14. - Small sessile droplet with shape of spherical segment.

graphical integration, was used to obtain the free surface area, as indicated in figure 13, from which

$$S \approx 2\pi \sum (y\,\Delta X) - \pi h \delta \tag{11}$$

The volume of a sessile mercury droplet was determined from the weight to density ratio w/ρ and was also calculated by equation (12), which was derived from the geometry of a small sessile droplet with the shape of a spherical segment, such as that shown in figure 14, where dA is a differential element of droplet area

$$dv = dA\,dr$$

Integrating the droplet volume gives

$$\left.\begin{aligned} v &= \int_{\varphi=0}^{\varphi=\theta_s} \int_{r=0}^{r} 2\pi r^2 \sin\varphi\, d\varphi\, dr \\ &= \int_0^{\theta_s} 2\pi \sin\varphi\, d\varphi \int_0^{r} r^2\, dr \\ &= 2\pi(1 - \cos\theta_s)\frac{r^3}{3} \\ &= \frac{\pi}{12}\delta^3(1 - \cos\theta_s) \end{aligned}\right\} \tag{12}$$

Mercury-Glass Thermal Equilibrium Time

Numerous investigators (e.g., refs. 3 and 8) have observed that the contact angle of

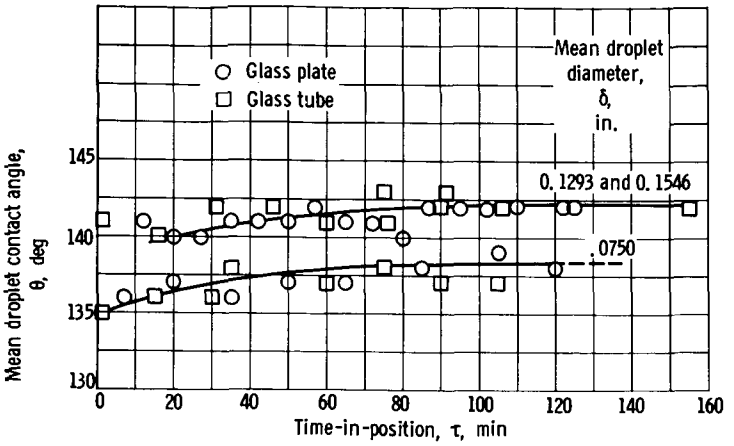

Figure 15. - Mean droplet contact angle as function of time-in-position.

a droplet on a solid surface in air increased slightly with time-in-position. It was therefore considered prudent for validation of droplet shape and contact angle data to define the equilibrium time requirements of the liquid-solid system used in this investigation.

When a mercury droplet was initially placed on the glass surface, a high degree of droplet surface oscillation was observed. Most likely this oscillation resulted from the internal molecular circulation, driven by a surface-tension gradient over the droplet surface due to temperature exchange between glass and mercury. When a mercury droplet was allowed to stay in position for a few minutes, it was observed that the droplet surface oscillation gradually decreased. Therefore, in order to determine the time required to attain thermal equilibrium between glass and a mercury droplet, ten mercury droplets varying in weight from 11.80×10^{-4} to 731.4×10^{-4} ounce were photographed at various times up to 155 minutes. The photographs of mercury droplets were taken in the glass tube and also on a horizontal glass plate. The mean contact angle of a sessile droplet in a glass tube and on glass plate was measured directly from enlarged photographs (magnification of 6) and also was calculated from the measured droplet dimensions. The results thus obtained of three representative droplets are shown in figure 15. Depending on droplet volume, the thermal equilibrium (zero change in contact angle with time) between glass and mercury was attained within a time interval of 60 to 80 minutes. All data in this investigation were taken at thermal equilibrium conditions. In the droplet size range analyzed, the effect of time-in-position on contact angle was the same for the glass plate and the glass tube.

Effect of Aberration

It is a well-known fact that the effect of refraction through one or more parallel-sided slabs displaces an image laterally but does not deviate from its true shape. How-

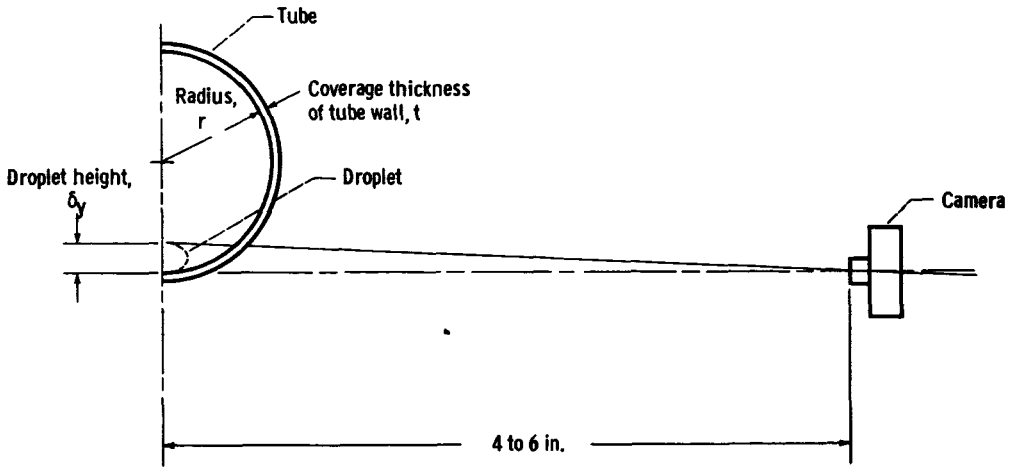

Figure 16. - Relative geometry of location of glass tube, droplet, and camera.

ever, the photographs of mercury droplets in a glass tube were taken through a curved tube wall. Therefore, in a plane normal to the length of the tube, the curvature of the tube wall at which light incidence from the camera film plane to a droplet varies from point to point. As shown in figure 16, the curvature of tube is concave inward; therefore, the change in curvature resulted in attenuation of droplet image on a camera screen. It was therefore desirable to determine the significance of the aberration effect on the results.

From the relative position of the tube, the droplet, and the camera, the droplet height attenuation δ_y was approximated by the following equation, which was derived from basic optics laws,

$$\Delta\delta_y = t \cos \varphi_i \left\{ \tan \varphi_i - \tan \left[\sin^{-1} \left(\frac{\mu_{air}}{\mu_{glass}} \sin \varphi_i \right) \right] \right\} \tag{13}$$

where φ_i is the angle of incidence, $\approx 1^o$ (for droplet of maximum size); μ_{air} is the absolute refractive index of air, ≈ 1.00; μ_{glass} is the absolute refractive index of glass, ≈ 1.50; and t is the estimated coverage thickness of a tube wall, ≈ 0.067 inch. By substituting these values into equation (13), the maximum possible attenuation of droplet height is $\approx 4.5 \times 10^{-4}$ inch, which is very small relative to droplet size. Since it is believed that equation (13) gives a reasonable approximation to the attenuation effect, the effect of refraction or aberration was neglected in the interpretation of photographic data.

All experiments in this study were conducted at ambient conditions. The ranges of variation of temperature, pressure, and relative humidity were as follows:

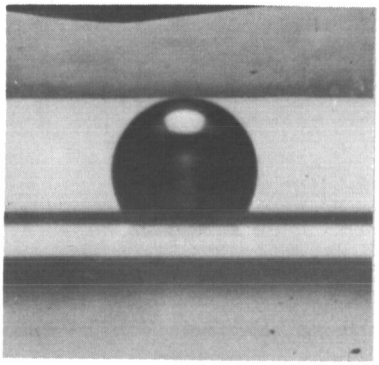

(a) Zero gravity.

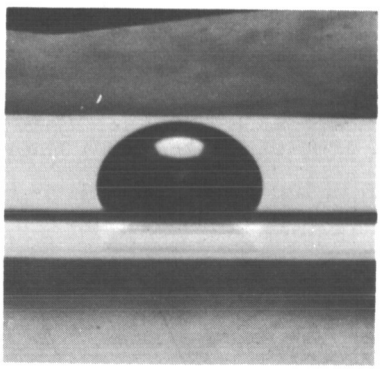

(b) 1 g.

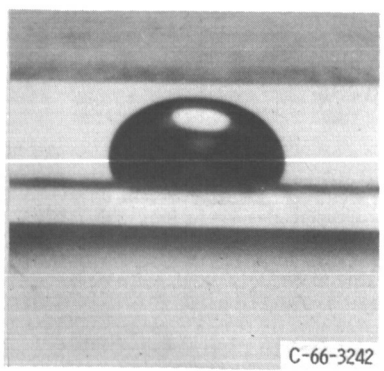

(c) $1\frac{1}{2}$ g's.

Figure 17. - Variation of mercury droplet shape with gravity level (gravity vector is normal to tube wall). Droplet weight, 12.26×10^{-3} ounce. X5.1.

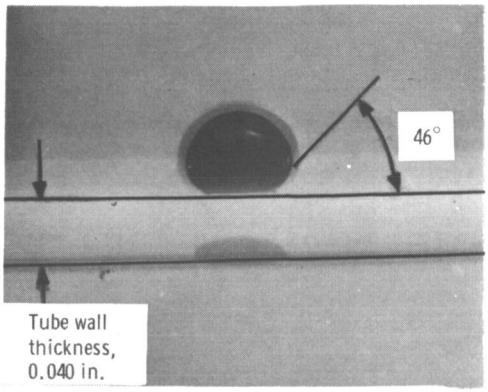

(a) Mean droplet diameter, 0.0723 inch.

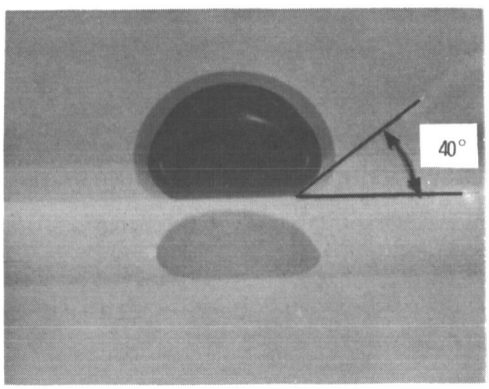

(b) Mean droplet diameter, 0.1157 inch.

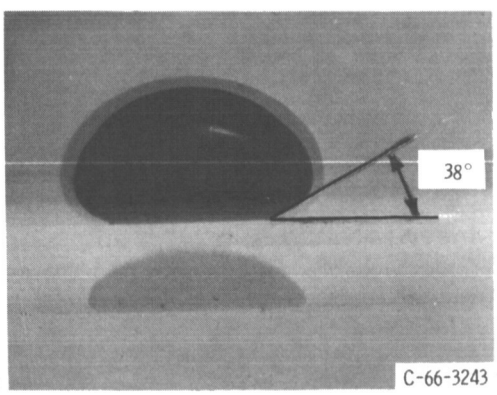

(c) Mean droplet diameter, 0.1548 inch.

Figure 18. - Variation of mercury droplet contact angle with size in horizontal glass tube (inside diameter 0.429 in.) in 1-g environment. X8.65.

Temperature, ^{o}F	75 to 82
Atmospheric pressure, in. of Hg	29.90 to 29.91
Relative humidity, percent	55 to 65

Therefore, it is believed that the effect of variation of the atmospheric conditions on the results presented in this report is negligible.

RESULTS AND DISCUSSION

In order to arrive at a means for predicting heat-transfer and pressure-drop characteristics of condensers operating in a nonwetting condition, it is necessary to define pertinent geometric characteristics of droplets such as surface areas, contact areas (with a tube wall), and droplet volumes. It would, therefore, be convenient to derive expressions for these geometric characteristics in terms of an easily identified variable that would yield valid results over a broad range of drop sizes under various gravity environmental operating conditions. This easily defined variable is drop diameter. However, the geometric characteristics of droplets in contact with a surface cannot be directly obtained from the drop diameter since these characteristics are functions of drop shape that, in turn, is a function of the contact angle. It is then necessary first to define the effects of droplet size and gravity environment on droplet shape and contact angle and then to relate, through the empirical expressions, the variations of drop geometry with drop diameter. The following discussion deals with experimentally and analytically defined contact angles and associated geometric parameters of mercury droplets.

Droplet Geometry Effect of Gravity on Radius of Curvature

Study of enlarged mercury droplet photographs (such as those shown in figs. 17 and 18) taken in various gravity environments indicated that the shape and, therefore, the contact angle of a given size sessile droplet varied with the level of gravity. In the droplet size range analyzed (0.0610 in. $\leq \delta \leq$ 0.2365 in.) in a zero-gravity environment, the shape of droplets resembled a spherical cup. However, in a 1-g environment, for sessile droplets less than 0.0713 inch, the shape deviated little from a spherical cup. For larger droplets, the shape deviated from a spherical cup progressively with an increase in size due to droplet flattening. The variation of the shape of a droplet with size in a 1-g environment is illustrated in figure 18. As would be expected, a given droplet subjected to $1\frac{1}{2}$- and 2-g environments was increasingly flattened, and the shape of droplets resembled an ellipsoidal cup.

The change of the shape of a droplet in contact with a solid surface with varying level of gravity suggested application of the theory of Bashforth and Adams (ref. 3) for calculating droplet contact angle from the measured droplet dimensions. Those dimensions are the radius of curvature at the apex b (given by eq. (5)), derived in the section METHOD OF ANALYSIS, the height δ_y, and the mean droplet diameter δ. In accordance with the theory of Bashforth and Adams, the contact angle depends not only on droplet size but also on shape. Therefore, these three droplet dimensions were related to two dimensionless factors, droplet size factor $2\delta_y/\delta$ and droplet shape factor $\delta/2b$. For a given droplet, they both varied with gravity level. The droplet apex curvature is plotted as a function of mean droplet diameter in figure 19 for different gravity levels. The apex curvature increases with an increase in droplet size. It is important to note that, for a given droplet volume, the mean diameter changes with gravity level, and it is therefore necessary to interpret effects of gravity level on droplet characteristics on the basis of droplet volume rather than droplet diameter (see bottom data). A digital computer program using a least-square-method curve fit for various droplet parameters produced an exponential equation in the form $\xi = B_1\delta + B_2 e^{(B_3\delta + B_4 n)}$ where ξ is a geometric droplet parameter, while B_1, B_2, B_3, and B_4 are constants determined empirically. Details of this program are described in reference 9.

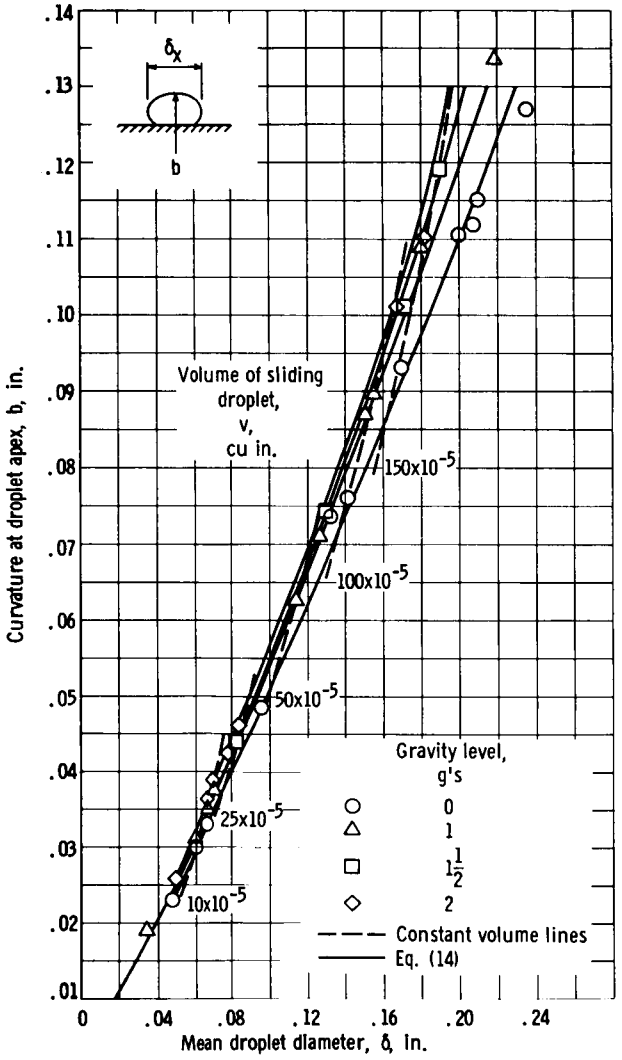

Figure 19. - Variation of curvature at droplet apex with droplet size for various gravity environments.

The general empirical equation obtained to express droplet curvature at its apex in the gravity environments and droplet size range investigated is

$$b = 0.544\,\delta + 0.112\times10^{-2}\, e^{(5.985\,\delta + 0.662\,n)} \qquad (14)$$

The accuracy of b obtained from equation (14) is within 0.50 percent relative to the values obtained from equation (5).

As shown in figure 15 (p. 14), a change in curvature is very sensitive to a change

in diameter. In the small droplet size range, $\delta \leq 0.0650$ inch, the change in curvature is negligible when going from one gravity level to the other; however, the effect of gravity on droplet curvature increases with an increase in droplet size.

Effect of Gravity on Droplet Height

The variation of the height of a sessile droplet in a glass tube with mean diameter for various gravity environments is presented in figure 20. In a given gravity field, the droplet height increases almost linearly with an increase in mean droplet diameter. In the range of droplet size and the environment of gravity investigated, the height of a sessile droplet in a glass tube can be expressed by the following empirical equation:

$$\delta_y = 0.234 \times 10^{-2} e^{(6.135\, \delta^{0.244} - 0.124\, n)} \qquad (15)$$

The accuracy of δ_y obtained from equation (15) is within 0.70 rms percent relative to the measured data points presented in figure 15 (p. 14). Equation (15) is valid in any gravity level investigated.

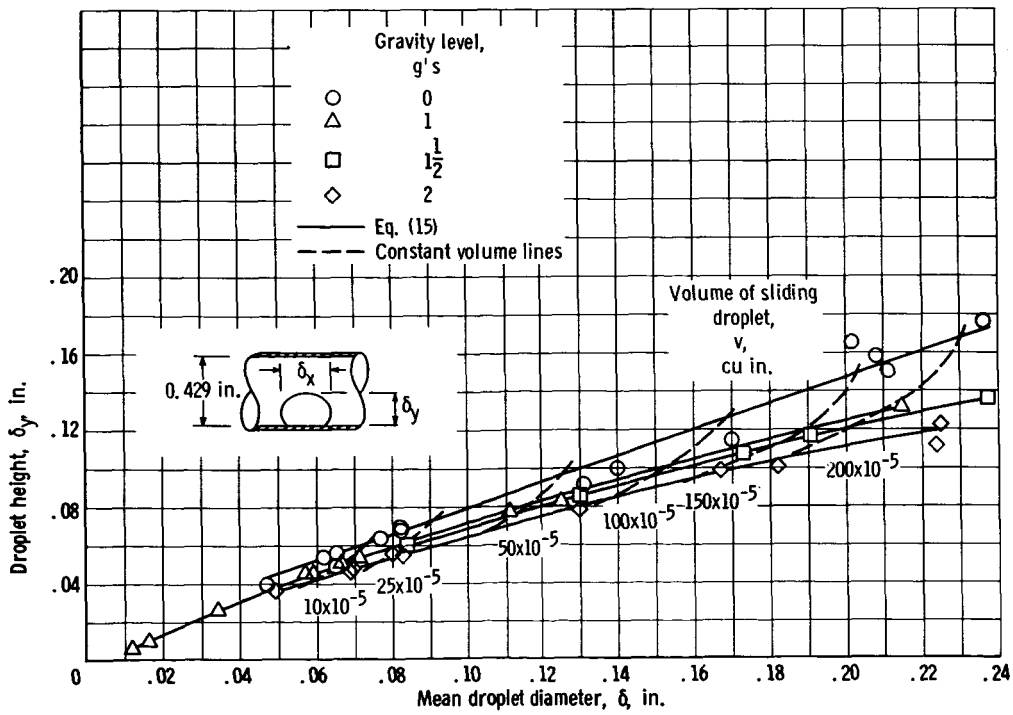

Figure 20. - Droplet height as function of mean droplet diameter.

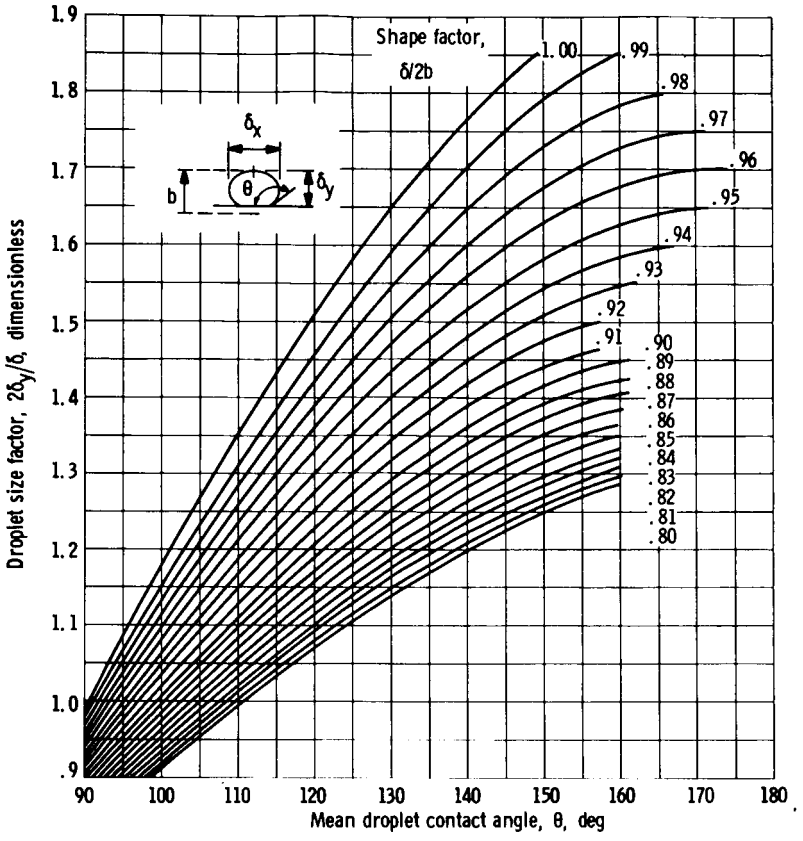

Figure 21. - Droplet size factor as function of mean contact angle.

Contact Angle

Calculated from droplet dimensions. - The original tables of Bashforth and Adams given in reference 3 provided the necessary information to produce figure 21. Here curves serve for determining contact angle by graphical interpolation from measured droplet dimensions. Dimensions have been selected that may be measured most precisely or which may be readily calculated from other experimental data. The most easily measured dimensions of a sessile droplet, as represented in the sketch in figure 21, are the total height and the mean diameter. These two dimensions determine the size of the droplet. However, the contact angle depends not only on the size of the droplet but also on its shape. Therefore, the contact angle of a droplet has been related not just to droplet size but also to its shape factor $\delta/2b$, which contains the radius of curvature b at the apex of the droplet.

For each value of $\theta_{s,c}$, the corresponding values of $2\delta_y/\delta$ and $\delta/2b$ were obtained by the numerical interpolation of the original Bashforth and Adams tables given in reference 3. The results obtained are presented in figure 21. The values of $\theta_{s,c}$ in this

figure are correct to the nearest 0. 1° relative to the original tables given in reference 3.

Direct measurement. - The data obtained by the direct measurement of contact angle of droplets from enlarged photographs are given in tables I to VI. In a non-zero-gravity environment, the mean contact angle increased with the mean droplet diameter until a maximum equilibrium value was reached. At this point, the contact angle became a constant independent of droplet size. The data obtained by direct measurement were less consistent than the data calculated from measured droplet dimensions. This inconsistency was attributed to irregularities in the glass surface or inherent human error of measurement, or both

Comparison of measured and calculated values. - The mean contact angle of a sessile droplet with a glass tube in various gravity environments was determined in two different ways: first, by the direct contact angle measurement at two points from the enlarged pictures of a droplet image, and second, from the measured dimensions of a droplet by the numerical interpolation of the Bashforth and Adams tables. The mean contact angle obtained is given in tables I to IV, and the correlation of calculated contact angles $\theta_{s,c}$ with the measured values $\theta_{s,m}$ are plotted in figure 22. The solid line in this figure represents the least-squares fit, and the dashed lines indicate a confidence band within ±2 percent deviation from the least-squares fit. It can be seen from this plot that 93 percent of all data points obtained in various gravity measurements fall within the confidence band.

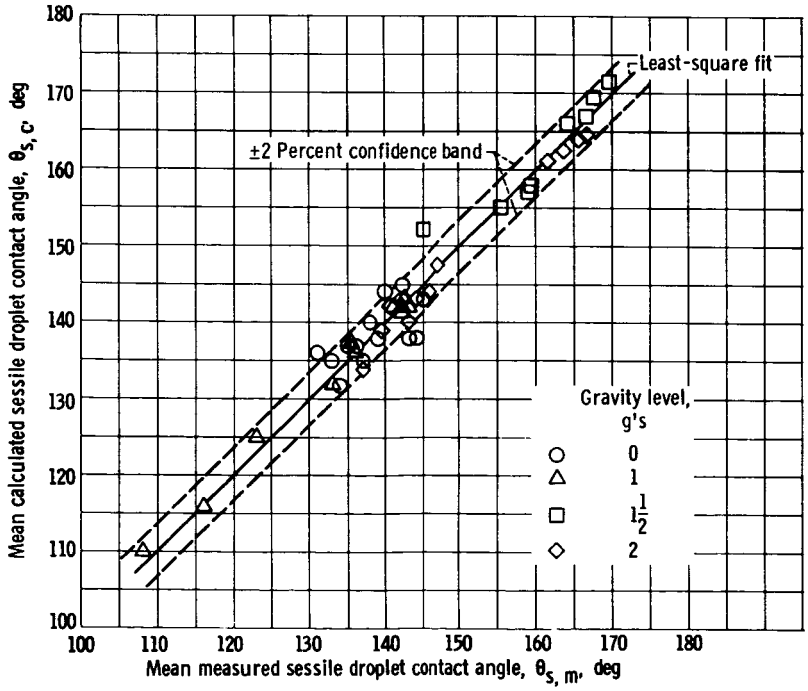

Figure 22. - Correlation of calculated contact angle of droplet with measured values for various environments of gravity.

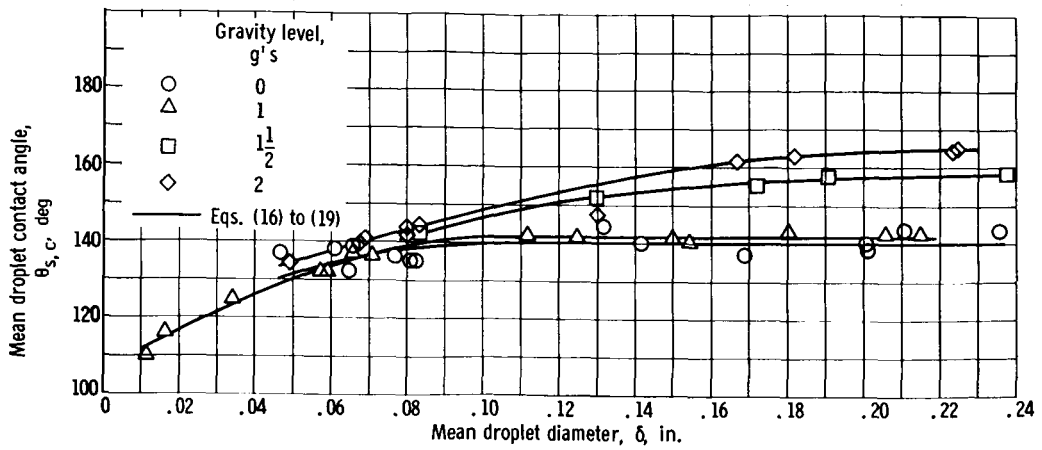

Figure 23. - Mean contact angle as function of mean droplet diameter.

Effect of droplet size. - In a given gravity environment, the contact angle formed by a sessile droplet on a solid surface depends on the droplet size and solid surface orientation in the gravity field. The variation of mercury droplet contact angle with its size in a 1-g environment is shown in figure 18 (p. 16). The values of mean contact angle corresponding to various droplet diameters and gravity fields are given in tables I to IV, and the results of mean contact angle $\theta_{s,c}$ as a function of droplet size δ are plotted in figure 23. In a 1-g environment, the mean contact angle of a droplet increases with the diameter until it approaches a maximum equilibrium value of 142° at a droplet size of 0.1122 inch (see table II).

The mean contact angle of a sessile droplet in a glass tube in 0-, 1-, $1\frac{1}{2}$-, and 2-g environments has been expressed by the following empirical equations;

$$\left(\theta_{s,c}\right)_0 = 134.254\, e^{0.244\,\delta} \qquad 0.0470 \text{ in.} \leq \delta \leq 0.0826 \text{ in.} \tag{16}$$

$$\left(\theta_{s,c}\right)_1 = 129.605\, e^{0.497\,\delta} \qquad 0.0116 \text{ in.} \leq \delta \leq 0.1122 \text{ in.} \tag{17}$$

$$\left(\theta_{s,c}\right)_{1\frac{1}{2}} = 141.697\, e^{0.478\,\delta} \qquad 0.0835 \text{ in.} \leq \delta \leq 0.2380 \text{ in.} \tag{18}$$

$$\left(\theta_{s,c}\right)_2 = 129.845\, e^{1.113\,\delta} \qquad 0.0491 \text{ in.} \leq \delta \leq 0.2250 \text{ in.} \tag{19}$$

Equations (16) to (19) are valid for the droplet size range indicated within an accuracy of 1.3, 2.3, 2.9, and 2.6 rms percent, respectively, relative to the calculated values from droplet dimensions. By introducing a gravity factor n, a general empirical equa-

tion was obtained from the data to express the mean contact angle of a sessile droplet for the range of gravity environment and droplet size investigated. Thus,

$$\theta_s = 1.167\, e^{\left(4.980\, \delta^{0.022} + 0.059\, n\right)} \tag{20}$$

The accuracy of θ_s obtained from equation (20) is within 8.0 rms percent relative to the data points presented in figure 23 in the gravity-levels investigated.

Effect of gravity. - Mean contact angles of various size sessile droplets were determined both by direct measurement and by computation from droplet geometry. All the data and calculated results are tabulated in tables I to IV.

In the droplet size range analyzed (0.0470 in. $\leq \delta \leq$ 0.2365 in.), the contact angle formed by a droplet and a glass tube in a zero-gravity environment varied little with droplet size. The data of mean calculated contact angle $\theta_{s,c}$ spread in a 7^o band. A plot of equation (16) in figure 23 represents the least-squares fit for all the calculated mean contact angles obtained in a zero-gravity environment. The contact angle increased slightly as droplet size increased. For example, for droplet diameter δ = 0.050 inch, $\theta_{s,c} = 131^o$, and for $\delta \geq$ 0.120 inch, the contact angle approaches a constant value of 140^o. The increase in contact angle with droplet size is attributed to the fact that, in general, the magnitude of surface tension of a liquid decreases with droplet size (ref. 10), and the contact angle for a given condition is directly proportional to the magnitude of surface tension. As shown in table I, the root-mean-square value of the mean calculated contact angle $\theta_{s,c}$ is 139^o in a zero gravity environment.

The surface tension of triple distilled mercury used in this analysis is about 0.03188 pound per foot at 70^o F. Then the average force of adhesion in the contact periphery of a droplet, as given by the following expression (ref. 10),

$$\Phi = \delta(1 + \cos\, \theta_{s,c})$$

is of the order of 0.00746 pound per foot. Because of the adhesion force, mercury droplets were observed to remain attached to the glass surface in a zero-gravity environment, as shown in figure 17 (p. 16).

In a 1-g environment, the droplet size range analyzed was 0.0116 inch $\leq \delta \leq$ 0.2150 inch. The calculated and measured mean contact angles $\theta_{s,c}$ and $\theta_{s,m}$ are given in table II, and the variation of calculated contact angle $\theta_{s,c}$ with droplet size δ is shown in figure 23. The effect of gravity on a contact angle of small droplets is negligible. However, as droplet size increased, the gravity effect on contact angle became significant. For example, for a droplet size δ of 0.050 inch, the contact angle changed by only a fraction of a degree by going from a zero-gravity to a 1-g environment; however, for a droplet size δ of 0.120 inch, the difference increased to 3^o for the same change in the environment of gravity.

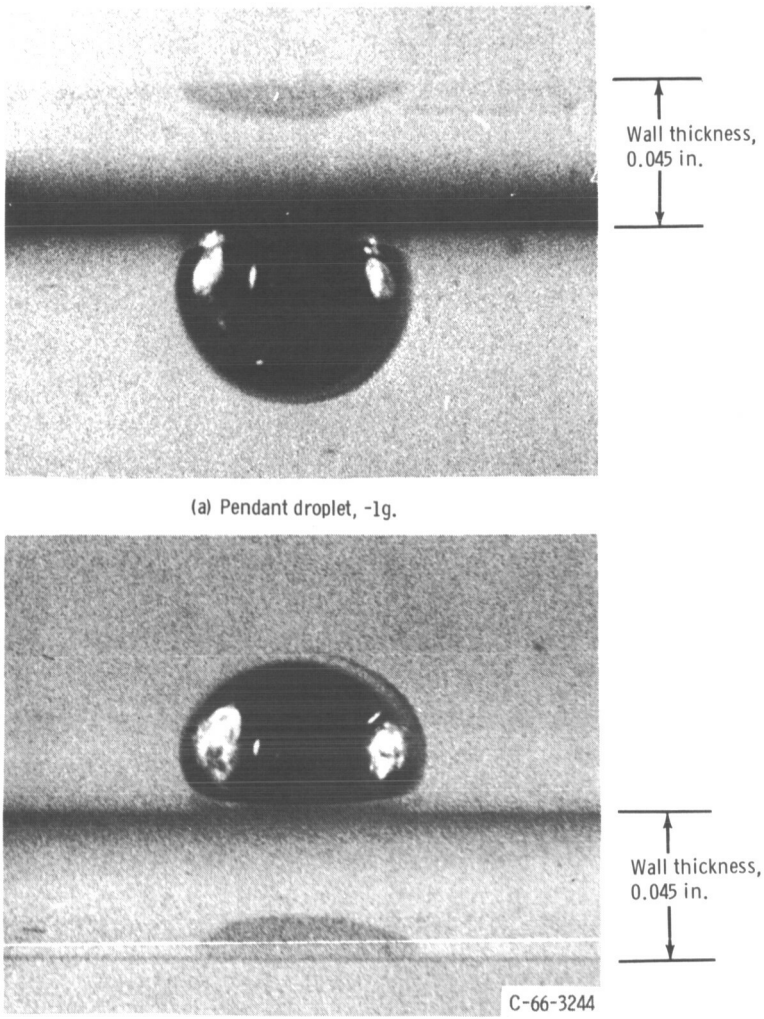

(a) Pendant droplet, -1g.

(b) Sessile droplet; 1 g.

Figure 24. - Gravity effect on mercury droplet shape. Droplet weight, 11.792×10^{-2} ounce. Force of adhesion, which holds attached droplet to glass surface, in periphery of pendant droplet is at least 0.00895 pound per foot. X15.1.

In a $1\frac{1}{2}$-g environment, the droplet size range analyzed was 0.0835 inch $\leq \delta \leq$ 0.3840 inch. The mean contact angles $\theta_{s,c}$ and $\theta_{s,m}$ obtained are given in table III, and the results of $\theta_{s,c}$ are plotted as a function of δ in figure 23. The gravity effect on a mean contact angle increased rapidly with an increase in droplet size. For example, for a mean droplet diameter of 0.0835 inch, the calculated mean contact angle is 143°, and for a mean droplet diameter of 0.1200 inch, the calculated mean contact angle is 150°. As shown in figure 23, the mean contact angle of a droplet approached a constant value of 157° at a droplet size of approximately 0.2000 inch.

Table IV contains calculated and measured data of the mean contact angle of droplets in the size range of 0.0491 inch $\leq \delta \leq$ 0.2250 inch. The calculated contact angles from the dimensions of droplets are more consistent than the measured values. Therefore, the calculated contact angles of sessile droplets are plotted as a function of droplet diameter in figure 23. The calculated contact angle of a sessile droplet in a 2-g environment varied from 134° for a mean droplet diameter of 0.0491 inch to 164.5° for 0.2250 inch, which is the maximum constant contact angle attained in this gravity environment.

In order to illustrate the presence of an adhesion force between glass and mercury and also to show the effect of gravity on a droplet shape and its contact angle, a mercury droplet (11.792×10^{-2} oz) was photographed in a pendant and in a sessile position. The pendant position of a droplet was obtained by rotating the glass tube 180° relative to the position of a sessile droplet. The enlarged photographs are shown in figure 24.

In the pendant position, the droplet was under the influence of a negative gravity and remained attached to the glass by adhesion force. The mean contact angle was 136°, and the dimensions of the droplet were a diameter of 0.0743 inch and a height of 0.0537 inch. The same sessile droplet in a positive gravity position exhibited a mean contact angle of 133°, a diameter of 0.0786 inch and a height of 0.0456 inch.

Geometric Characteristics of Droplet

Those parameters such as droplet contact diameter with tube wall droplet height, droplet contact area with tube wall, droplet surface area exposed to vapor phase, and droplet volume were obtained from experimental measurements. Each geometric parameter was plotted as a function of mean droplet diameter and expressed by an empirical equation for each gravity level considered. The use of the digital-computer least-squares program was employed to obtain empirical equations for each geometric parameter analyzed.

Contact diameter. - The variation of true contact diameter on the tube wall of a sessile droplet with mean diameter is presented in figure 25. The droplet true contact diameter increases almost linearly with an increase in droplet mean diameter. In the range

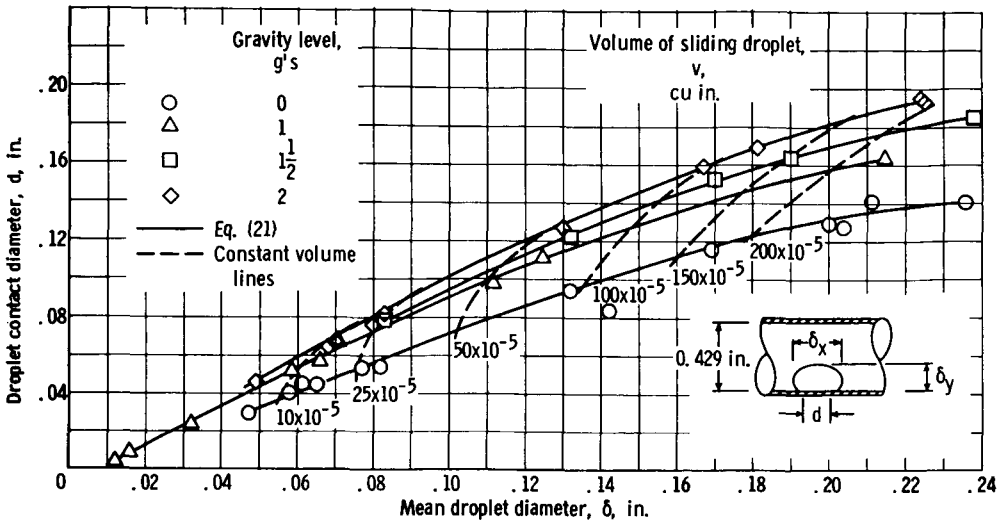

Figure 25. - Droplet contact diameter as function of mean droplet diameter measured in glass tube.

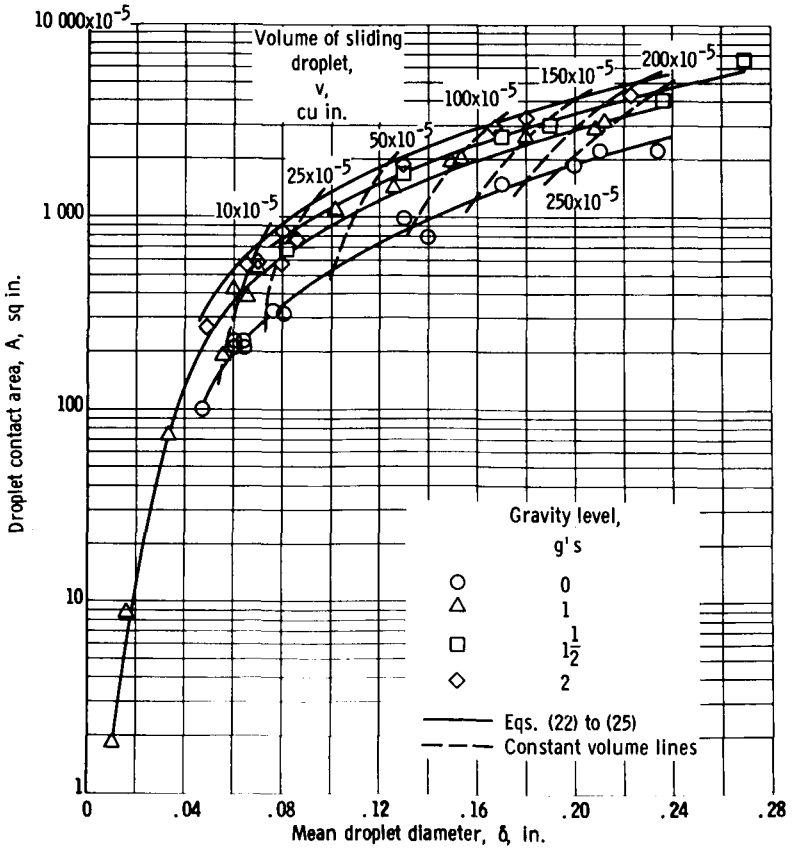

Figure 26. - Correlation of measured droplet contact area with tube wall to calculated values from equations (22) to (25).

of gravity environment and droplet size investigated, the true contact diameter of a sessile droplet with tube wall can be expressed by the following empirical equation:

$$d = (0.408\,\delta - 0.0198)e^{0.179\,n} \tag{21}$$

The accuracy of d obtained from equation (21) is within 0.70 rms percent relative to the measured data presented in figure 25.

Contact area. - The measured values of contact area of a sessile droplet with tube wall for various gravity environments are shown as a function of a mean droplet diameter in figure 26. The values for the droplet contact area correction factor are presented in tables I to IV. The numerical values of the root mean square of F were 1.40, 1.41, 1.42, and 1.50 for gravity levels of 0, 1, $1\frac{1}{2}$, and 2, respectively. Therefore, using equation (9) and the expression for d given by equation (21) results in the following empirical equations for the contact area of a sessile mercury droplet with the tube wall for 0-, 1-, $1\frac{1}{2}$-, and 2-g environments, respectively:

$$A_0 = 1.40\,\frac{\pi}{4}\,(0.408\,\delta - 0.0198)^2 \tag{22}$$

$$A_1 = 1.41\,\frac{\pi}{4}\,(0.408\,\delta - 0.0198)^2 e^{0.179} \tag{23}$$

$$A_{1\frac{1}{2}} = 1.42\,\frac{\pi}{4}\,(0.408\,\delta - 0.0198)^2 e^{0.537} \tag{24}$$

$$A_2 = 1.50\,\frac{\pi}{4}\,(0.408\,\delta - 0.0198)^2 e^{0.716} \tag{25}$$

Equations (22) to (25) are valid in the droplet size range indicated in tables I to IV, within an approximate accuracy of 1.04, 1.68, 2.01, and 2.42 rms percent, respectively, relative to the values measured with the planimeter. The data obtained are listed in tables I to IV. The calculated and measured results presented in figure 26 indicate the variation of droplet contact area on the tube wall with droplet diameter. Droplet constant volume shown by the dashed lines indicates that, for a given volume, the droplet mean diameter and consequently the droplet contact area increases with increased gravity level.

Surface area. - The values of the free surface area obtained from equations (10) and (11) for the range of droplet sizes and gravity environments are given in tables I to IV, and the results are plotted as a function of mean droplet diameter in figure 27. In

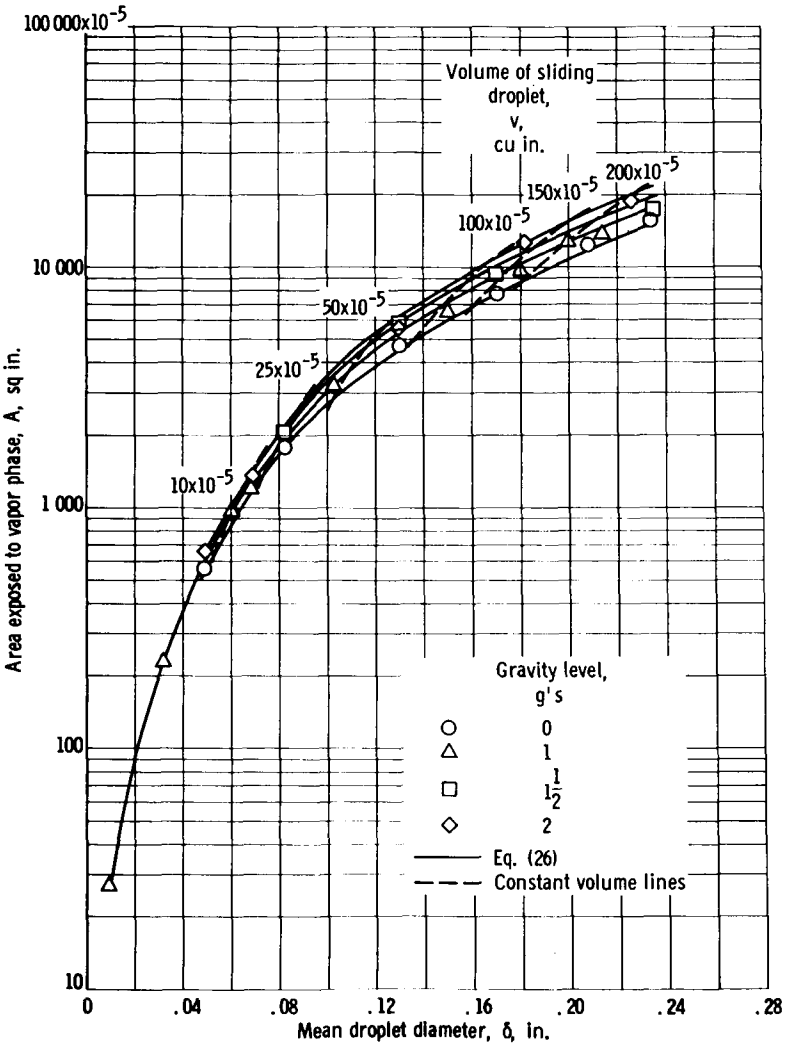

Figure 27. - Variation of droplet surface area exposed to vapor phase with mean droplet diameter for various gravity environments. (Data obtained by using eqs. (10) and (11).)

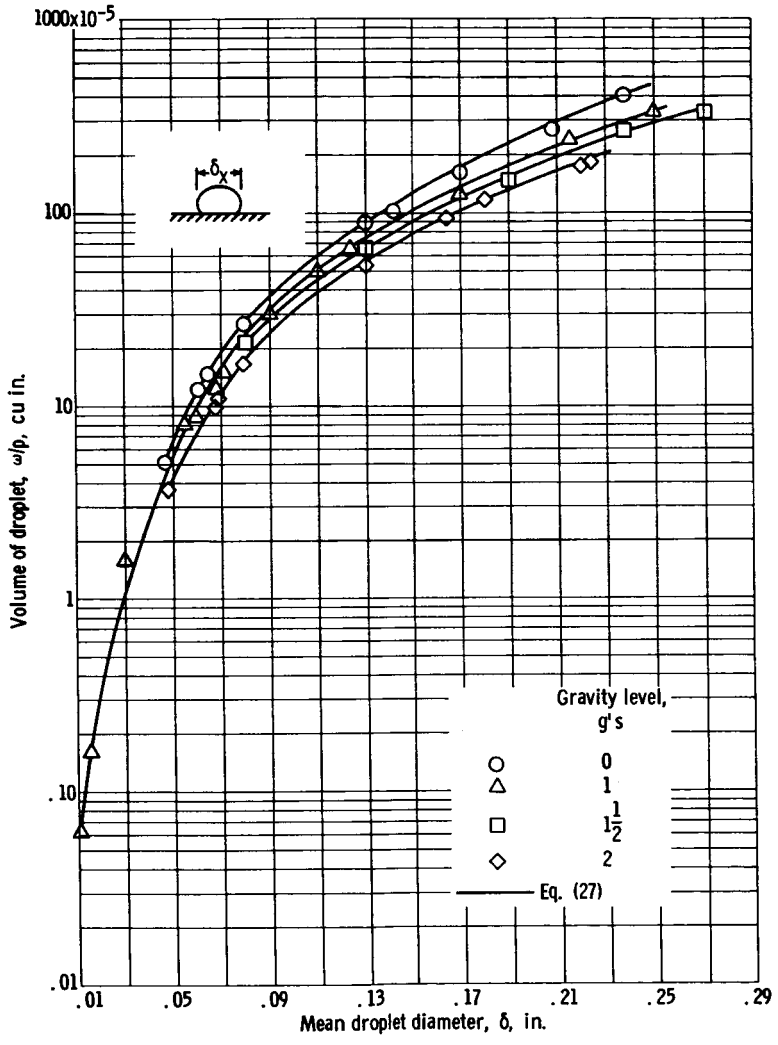

Figure 28. - Volume of sessile droplet as function of mean droplet diameter.

the range of droplet size and gravity level analyzed, the free surface area of a sessile droplet in a glass tube has been expressed by the following empirical equation:

$$S = 0.2884 \times 10^{-5} e^{(18.1082 \delta + 2.7699 n)} + 2.8594 \delta \quad (26)$$

This equation is valid in the droplet size range and gravity level investigated. The accuracy of S obtained from this equation is within 0.66 rms percent relative to the data presented in figure 27.

The free surface area of a droplet exposed to the vapor phase is dependent on droplet diameter. However, an appreciable change in droplet contact angle results in a little change in a droplet surface area. For example, for a 0.065-inch-diameter droplet, a change of 10° in contact angle results in approximately 10 percent change in surface area, as calculated from equation (10).

Volume. - The droplet volume w/ρ, determined experimentally, is plotted as a function of a mean droplet diameter in figure 28. The mean diameter of a given volume sessile droplet depends on gravity environmental conditions, as shown in figure 17 (p. 16). In addition, the variation of mean droplet diameter with the level of gravity is illustrated by constant volume lines in figures 19, 20, 25, 26, and 27, represented by dashed lines.

In the range of droplet size and gravity level investigated, the volume w/ρ of a sessile droplet in a glass tube is expressed by the following empirical equation:

$$v = 2018.566 e^{-(10.322 \delta^{-0.171} + 2.701 n)} \quad (27)$$

The accuracy of v obtained from this equation is within 0.83 rms percent of w/ρ.

Dynamic Contact Angle

The advancing θ_A and receding θ_R contact angles of a droplet sliding in an inclined glass tube undergo measurable changes with droplet velocity. These two contact angles of mercury droplets in the size range from 0.0375 to 0.2501 inch were measured at sliding velocities from 0 to 3.33 inch per second on enlarged photographs, such as that shown in figure 29. The data obtained are tabulated in tables V and VI, and the results are presented in figures 30 and 31.

The variation of θ_A, θ_R, and $\Delta\theta$ of a mercury droplet with mean diameter δ in an inclined glass tube at zero sliding velocity is tabulated in table V, and the results are plotted in figure 30. The droplet pictures were taken in an inclined glass tube at maximum droplet distortion 0.01° before movement.

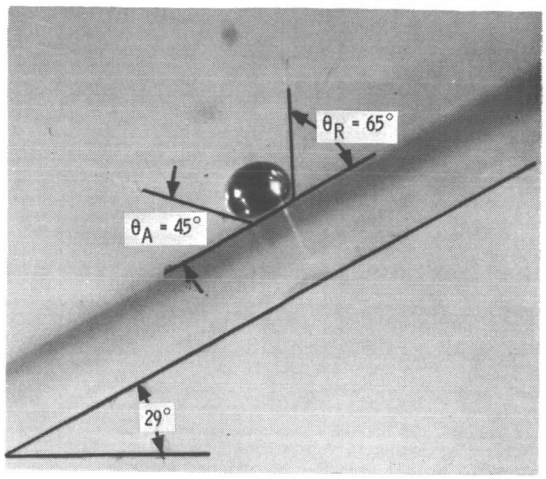

(a) Mean droplet diameter, 0.0375 inch.

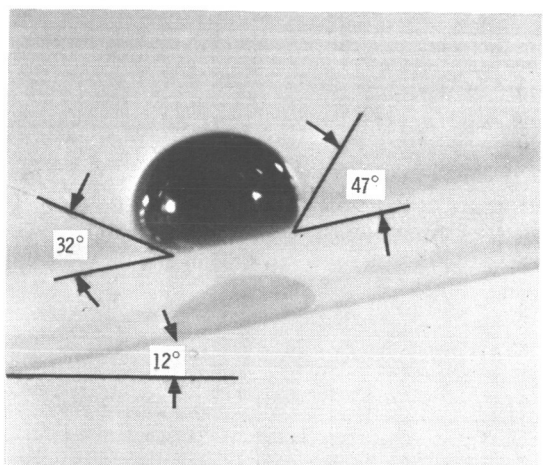

(b) Mean droplet diameter, 0.0875 inch.

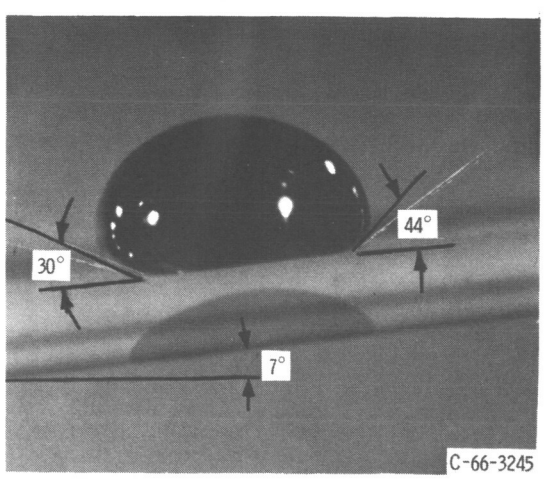

(c) Mean droplet diameter, 0.1128 inch.

Figure 29. - Distortion of mercury droplet contact angle ($\theta_A > \theta_R$) in inclined glass tube (inside diameter, 0.429 in.) for 1-g environment. Picture taken at instant when droplet started to slide. X9.7.

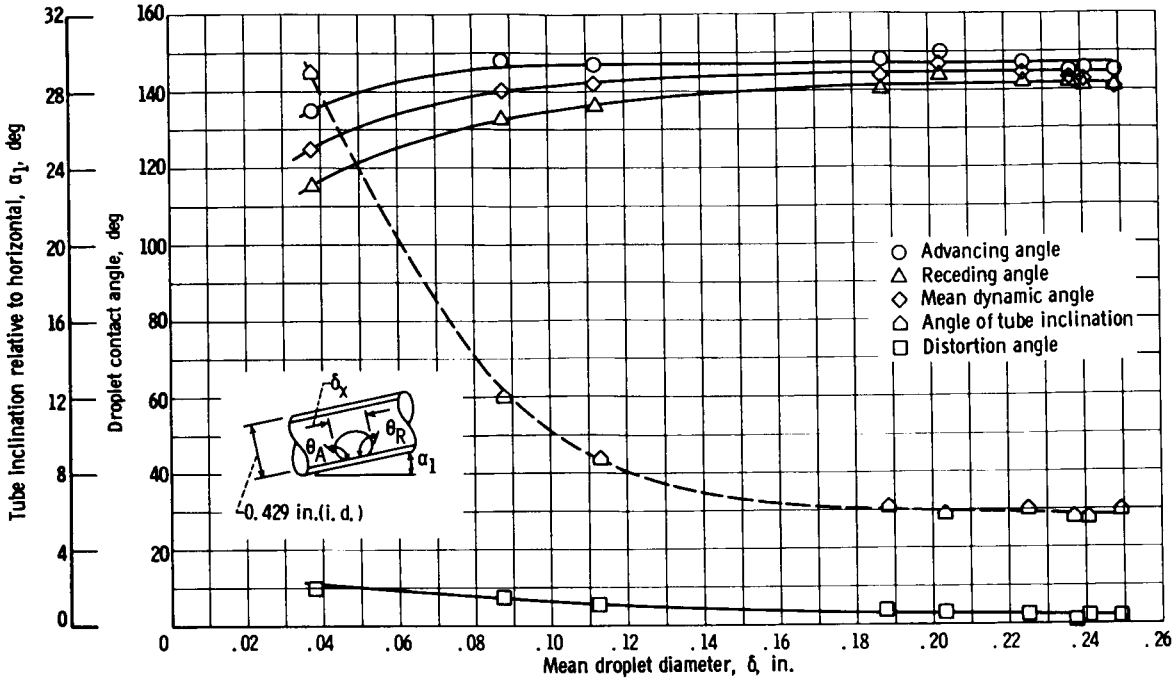

Figure 30. - Variation of dynamic angles of droplet with mean diameter in inclined glass tube at angle relative to horizontal (at zero droplet velocity).

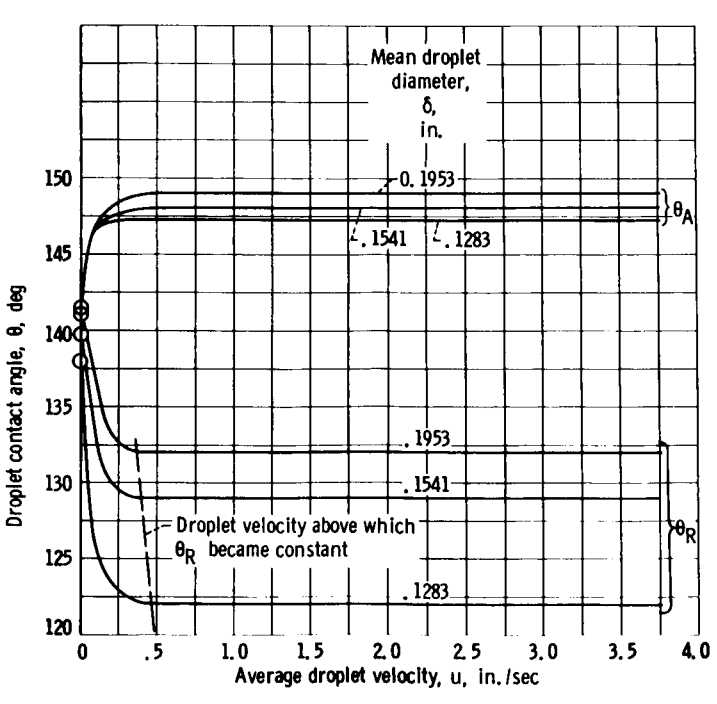

Figure 31. - Droplet contact angle as function of average velocity of droplet.

As shown in figure 30, at zero droplet velocity, the distortion contact angle $\Delta\theta$ decreased with an increase in droplet size. The advancing θ_A and the receding θ_R contact angles increased with an increase in droplet size, and also asymptotically approached a constant value of $\theta_A = 147^o$ and $\theta_R = 1.41^o$ at droplet sizes of 0.100 and 0.180 inch, respectively.

The variation of advancing θ_A, receding θ_R, and distortion $\Delta\theta$ contact angles with the droplet velocity are given in table VI and in figure 31. Up to a velocity of about 0.70 inch per second, the advancing contact angle increased and the receding contact angle decreased with droplet velocity, and above this rate, both angles approached a constant value. For a given droplet size, the advancing contact angle increased less than the receding contact angle relative to the mean contact angle at incipient movement. For example, for a droplet diameter of 0.1283 inch, moving with the average velocity 0.70 inch per second, θ_A was 147^o and θ_R was 123^o, while the incipient movement contact angle was 142^o.

SUMMARY OF RESULTS

A photographic study of mercury droplet parameters on a flat glass plate in 1-g environment, and also in a glass tube in 0-, 1-, $1\frac{1}{2}$-, and 2-g environments yielded the following results:

1. The contact angle of a sessile droplet was affected by its size and gravity environment. The contact angle increased with increase in gravity and by a greater amount for large droplets than for small droplets. Also the contact angle tended to maximize at larger droplet sizes as gravity level was increased.

2. In a 1-g environment, the maximum equilibrium contact angle was 142^o for droplet sizes greater than 0.1122 inch. In a zero-gravity environment, the maximum equilibrium contact angle was 139^o (rms).

3. In the range of droplet size and gravity level investigated, empirical equations were developed for expressing the geometric droplet parameters as a function of mean diameter including (1) mean contact angle, (2) contact diameter, (3) surface area, and (4) volume.

4. In a 1-g environment, tests showed that thermal equilibrium between glass and mercury at ambient conditions was attained within a time interval of 60 to 80 minutes.

5. In a 1-g environment, the dynamic contact angle of a droplet was affected by the droplet size and tube inclination relative to a horizontal. The value of mean contact angle

of a mercury droplet sliding under the influence of gravity in an inclined glass tube was approximately equal to a mean contact angle of a sessile droplet in a horizontal tube.

Lewis Research Center,
National Aeronautics and Space Administration,
Cleveland, Ohio, August 2, 1966,
701-04-00-02-22.

APPENDIX A

SYMBOLS

A	contact area of a droplet with solid surface, sq in.
A_{cir}	circular contact area calculated from minor axial droplet contact diameter
a	acceleration, ft/sec^2
b	curvature of sessile droplet at apex, in.
c^2	Laplacian capillary constant of sessile droplet, sq in.
d	contact diameter of sessile droplet with solid surface, in.
F	contact area correction factor, A_c/A_{cir}
f	measure of deviation of actual droplet shape from spherical, dimensionless
g	gravitational acceleration, ft/sec^2
L	length of major axis of ellipse of droplet in contact with tube wall, in.
n	gravity factor, a/g, dimensionless
r	radius, in.
S	surface area of a droplet exposed to vapor phase, sq in.
u	velocity, in./sec
v	volume, w/ρ, cu in.
w	weight, lb
x, y, z	Cartesian coordinates
α	maximum tube inclination before droplet motion, deg
β	ratio of $2b^2/c^2$, dimensionless
δ	mean diameter of droplet, in.
θ	mean contact angle of droplet, deg
$\Delta\theta$	distortion angle of droplet on inclined solid surface, $(\theta_A - \theta_R)/2$, deg
θ_A	advancing contact angle of droplet on inclined solid surface, deg
θ_d	mean dynamic contact angle of droplet on inclined solid surface, $(\theta_A + \theta_R)/2$, deg
θ_R	receding contact angle of droplet on inclined solid surface, deg
ρ	density, ft^3
σ	surface tension, lb/ft
τ	time-in-position of droplet on solid surface, min
Φ	adhesion force, lb/ft
φ	angle, degrees of liquid

Subscripts:

c	calculated
m	measured

s	sessile	1	1 g
v	vapor	$1\frac{1}{2}$	$1\frac{1}{2}$ g's
x, y, z	Cartesian coordinates	2	2 g's
0	zero gravity		

Conversion factors from English to Metric units

Multiply	By	To obtain
Inches	2.540	Centimeters
Square inches	6.452	Square centimeters
Feet per second per second	30.480	Centimeters per second per second
Pounds (force) per foot	145.936×10^2	Dynes per centimeter
Inch per second	2.540	Centimeter per second
Pounds per cubic foot	0.01602	Grams per cubic centimeter
$^{o}F - 32$	5/9	^{o}C

APPENDIX B

ZERO-GRAVITY AND MULTI-GRAVITY FACILITIES

The 0-, $1\frac{1}{2}$-, and 2-g gravity levels required for the tests were produced by using two different airplanes: some experiments were conducted with the AJ-2 shown in figure 32, while the others were conducted with the L-17, shown in figure 33.

A typical trajectory for the Lewis AJ-2 is shown in figure 34. This maneuver produces a theoretical maximum zero-gravity time of 24 seconds (fig. 35). The maneuver was entered from a dive, and the airplane was rotated at 400 knots true airspeed to arrive at a pitch angle of 42° with a speed of 310 knots true airspeed. Transition was made from a nominal 2-g pullup rotation to the zero-gravity condition where the airplane was flying on a Keplerian trajectory. Approximately 5 or 6 seconds were required for transition from the pullup to the zero-gravity condition, and a similar time was required at the exit of the Keplerian curve or pullout. These transition times reduce the theoretical maximum zero-gravity time to a practical time of 12 to 14 seconds.

The zero-gravity times obtained for this study were adequate, since droplet stabilization times in place were of the order of 3 to 4 seconds. The quality of the zero-gravity condition produced in the airplane should be considered on the basis of the three axes of measurement; however, the lateral and longitudinal accelerations always had a better

Figure 32. - AJ-2 Navy bomber converted to zero-gravity flight facility.

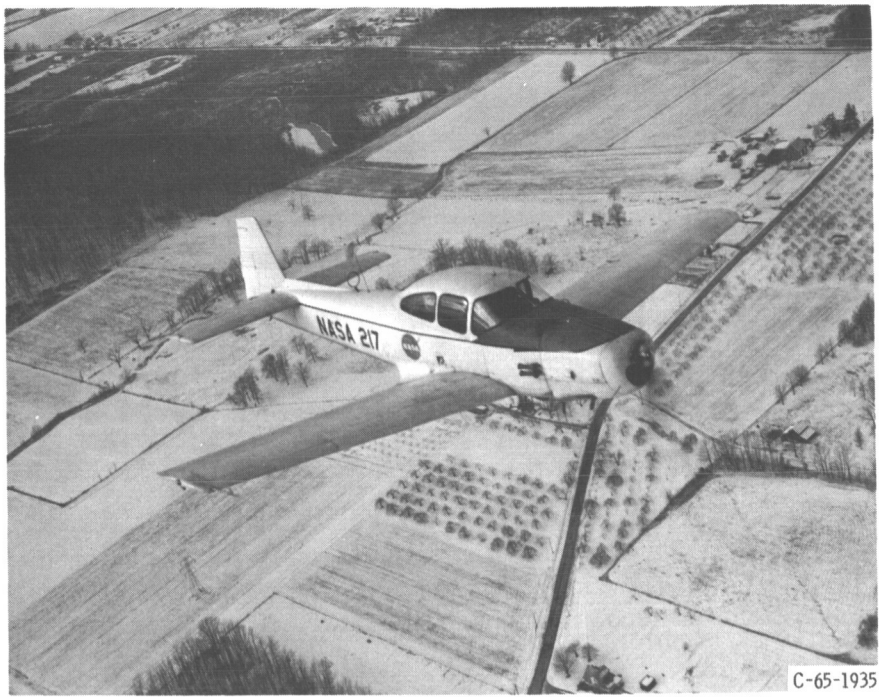

Figure 33. - Ryan L-17 airplane used to produce $1\frac{1}{2}$ - and 2-g gravity environments in circular trajectory.

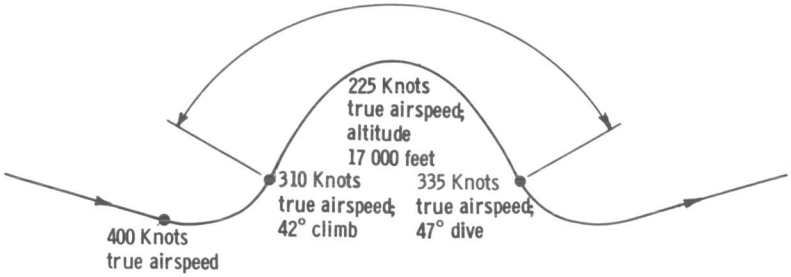

Figure 34. - Typical trajectory. Actual zero-gravity time, 12 to 14 seconds; theoretical maximum overall time, 24 seconds.

quality than the vertical acceleration. The vertical accelerations for a typical trajectory are shown in figure 35. During this maneuver, 2. 5 seconds were at a level of 0. 005 g or less, while 19. 1 seconds were at a level less than 0. 1 g.

All the maneuvers flown during the test program were analyzed, and the average zero-gravity times were computed. From these data it was shown that, for an average of 5. 28 seconds per trajectory, the gravity level was within ±0. 01 g, and for 12. 72 seconds the gravity level was within ±0. 05 g.

The gravity levels of $1\frac{1}{2}$ and 2 g's were produced by flying the airplane in a circular trajectory, such as that shown in figure 36. In this trajectory, the airplane was used as a large centrifuge, and gravity levels were produced for a period of 35 seconds (approxi-

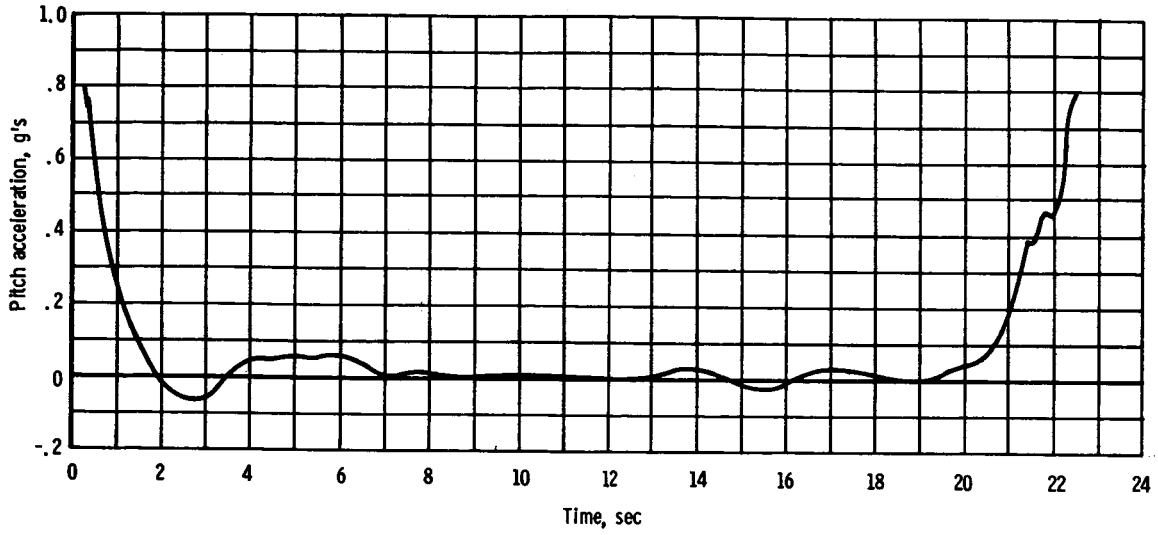

Figure 35. - Pitch acceleration during typical trajectory.

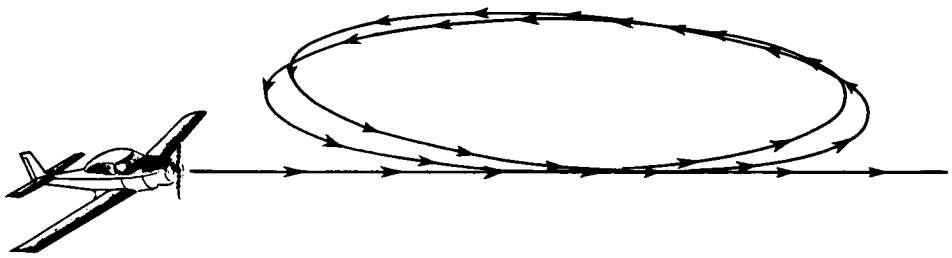

Figure 36. - Path of circular trajectory in which $1\frac{1}{2}$- and 2-g gravity levels were produced flying airplane centrifugally. (Orbits shown are displaced for illustration only.)

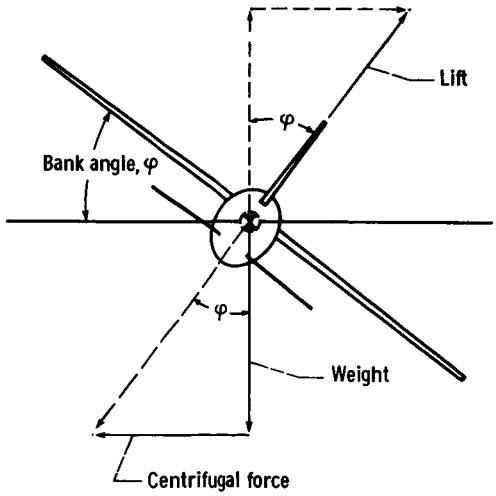

Figure 37. - Relation of forces acting on airplane flying centrifugally in steady turn.

mately) although no time limit is imposed by the aircraft as in zero gravity. During a steady nonslip or nonskidding turn, the lift will result in a horizontal component of a force, which in magnitude must be equal to the centrifugal force of the turn on the airplane. A steady turn of the airplane in a circular trajectory also produces a vertical component of lift equal to the weight of the airplane. The relation of forces acting on the airplane flying centrifugally in a steady turn is illustrated in figure 37. In order to produce a desired level of gravity in a plane of a centrifugal turn, the following force balance equation should be satisfied. Thus,

$$n = \frac{L}{W} = \frac{1}{\cos \varphi}$$

where n is the load factor, number of g's/g; W is the weight of airplane; and φ is the bank angle. It is apparent from this equation that for a steady, coordinated turn, a given load factor requires a specific bank angle, that is, 60° gives 2.0 g's, 70.5° gives 3.0 g's, etc. If the airplane were at a bank angle φ, and the lift was not provided to produce the correct load factor n, the airplane would accelerate in vertical and horizontal directions, and the turn would not be steady. Also, any side force on the airplane due to side slip would place the resultant aerodynamic force out of the plane of symmetry perpendicular to the airplane lateral axis and a lateral acceleration component would be present. In order to produce a steady turn in a circular trajectory, increased lift was required, which, in turn, produced an increase in total drag for the period of flight in the circular trajectory, because of the increased induced drag. Therefore, the thrust had to be increased to keep longitudinal airplane accelerations zero. Lateral accelerations were kept at zero by the pilot, using conventional aircraft instrumentation. The quality of $1\frac{1}{2}$- and 2-g gravity levels produced in the airplane flying in a circular trajectory were considered on the basis of the three axes of accelerometer measurements. The acceleration recorded in a plane of a typical circular trajectory flown for $1\frac{1}{2}$- and 2-g gravity levels were ± 0.10 g or better.

REFERENCES

1. Umur, Aydin: Mechanism of Dropwise Condensation. Ph. D. Thesis, Massachusetts Inst. of Tech., 1963.

2. Fatica, Nicholas; and Katz, Donald L.: Dropwise Condensation. Chem. Eng. Prog., vol. 45, no. 11, Nov. 1949, pp. 661-674.

3. Basforth, Francis: An Attempt to Test the Theories of Capillary Action by Comparing the Theoretical and Measured Forms of Drops of Fluid. Cambridge Univ. Press, 1883.

4. Mack, Guilford L.; and Lee, Dorothy A.: Determination of Contact Angles from Measurements of the Dimensions of Small Bubbles and Drops. II. The Sessile-Drop Method for Obtuse Angles. J. Phys. Chem., vol. 40, 1936, pp. 169-176.

5. Whetherford, W. D., Jr.; Tyler, John C.; and Ku, P. M.: Properties of Inorganic Energy-Conversion and Heat-Transfer Fluids for Space Applications. (WADD TR 61-96), Southwest Research Inst., Nov. 1961.

6. Rayleigh, Lord: On the Theory of the Capillary Tube. Roy. Soc. Proc., Ser. A, vol. 92, Jan. 1915, pp. 184-195.

7. Dorsey, N. Ernest: A New Equation for the Determination of Surface Tension from the Form of a Sessile Drop or Bubble. J. Wash. Acad. Sci., vol. 8, no. 19, Nov. 1928, pp. 505-509.

8. Marquardt, Donald W.: An Algorithm for Least-Squares Estimation of Nonlinear Parameters. Soc. Ind. Appl. Math. J., vol. 11, no. 2, June 1963, pp. 431-441.

9. Burdon, R. S.: Surface Tension and the Spreading of Liquids. Cambridge Univ. Press, 1940.

10. Miller, N. F.: The Wetting of Steel Surfaces by Esters of Unsaturated Fatty Acids. J. Phys. Chem., vol. 50, no. 4, July 1946, pp. 300-319.

11. Bartell, F. E.; and Cardwell, Paul H.: Reproducible Contact Angles on Reproducible Metal Surfaces. I. Contact Angles of Water Against Silver and Gold. Am. Chem. Soc. J., vol. 64, no. 3, Mar. 1942, pp. 494-497.

TABLE I. - PARAMETERS OF LIQUID MERCURY DROPLETS IN ZERO-GRAVITY ENVIRONMENT MEASURED IN 0.429-INCH INSIDE-DIAMETER GLASS TUBE

[Temperature, 82° F; relative humidity, 55 percent.]

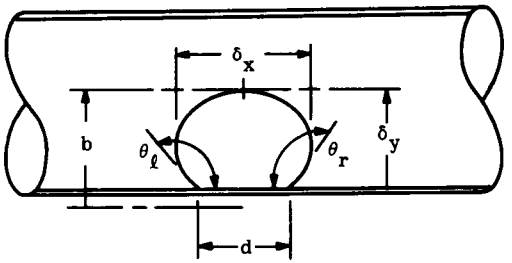

Droplet	Mean droplet diameter, δ, in.	Laplacian constant, c^2, sq in.	Size factor, $\frac{2\delta_y}{\delta}$	Shape factor, $\frac{\delta}{2b}$	Measured mean contact angle, $\theta_{s,m} = \frac{\theta_\ell + \theta_r}{2}$, deg	Calculated mean contact angle, $\theta_{s,c}$, deg	Free surface area (eq. (10)), S, sq in.	Free surface area (eq. (11)), S, sq in.	Measured tube-wall droplet contact area, A_c, sq in.	Contact area correction factor, $F = \frac{A_c}{A_{cir}}$	Contact area (eq. 21)), A, sq in.	Relative error in contact area, $\frac{A - A_c}{A_c} \times 100$, percent
1	0.0470	0.011313	1.710	0.995	135	137	600×10^{-5}	588×10^{-5}	336×10^{-5}	1.396	352×10^{-5}	4.80
2	.0610	.011280	1.760	1.000	139	138	1 032	----------	101	1.413	109	6.00
3	.0614	.011277	1.780	.995	136	137	1 030	----------	207	1.383	211	1.94
4	.0650	.011265	1.500	.964	134	132	1 128	----------	229	1.396	233	1.75
5	.0653	.011263	1.730	1.005	143	138	1 170	----------	227	1.383	230	1.32
6	.0770	.011220	1.680	.995	131	136	1 600	----------	335	1.397	370	10.50
7	.0816	.011233	1.710	1.000	133	135	1 767	----------	333	1.384	346	3.90
8	.0626	.011246	1.650	.995	137	135	1 823	$1\ 801\times10^{-5}$	208	1.384	237	13.90
9	.1320	.011163	1.380	.895	140	144	4 930	$4\ 870\times10^{-5}$	981	1.410	877	-.41
10	.1420	.011094	1.450	.930	138	140	5 575	----------	785	1.414	902	14.90
11	.1693	.011073	1.360	.910	135	137	7 775	$7\ 877\times10^{-5}$	1470	1.400	1466	-.27
12	.2030	.011008	1.621	.965	142	145	11 800	----------	1863	1.401	1860	-.16
13	.2080	.011003	1.460	.938	144	138	12 500	$12\ 483\times10^{-5}$	1800	1.385	1910	6.10
14	.2115	.011004	1.455	.915	142	140	12 400	----------	2175	1.410	2188	.59
15	.2365	.011001	1.464	.928	147	143	16 400	$16\ 305\times10^{-5}$	2175	1.410	2430	12.20
Root-mean-square value					139					1.40		7.15

TABLE II. - PARAMETERS OF LIQUID MERCURY DROPLETS[a] IN 1-g ENVIRONMENT (GROUND TEST) MEASURED IN 0.429-INCH INSIDE-DIAMETER GLASS TUBE

[Temperature, 81° F; relative humidity, 60 percent.]

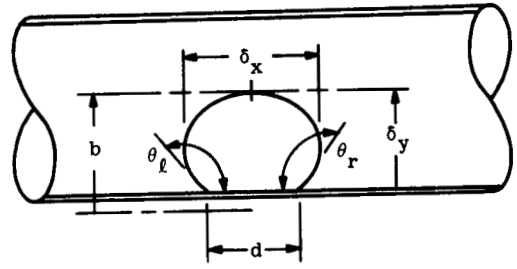

Droplet	Mean droplet diameter, δ, in.	Laplacian constant, c^2, sq in.	Size factor, $\frac{2\delta_y}{\delta}$	Shape factor, $\frac{\delta}{2b}$	Measured mean contact angle, $\theta_{s,m} = \frac{\theta_\ell + \theta_r}{2}$, deg	Calculated mean contact angle, $\theta_{s,c}$, deg	Free surface area (eq. (10)), S, sq in.	Free surface area (eq. (11)), S, sq in.	Measured tube-wall droplet contact area, A_c, sq in.	Contact area correction factor, $F = \frac{A_c}{A_{cir}}$	Contact area (eq. (22)), A, sq in.	Relative error in contact, area, $\frac{A - A_c}{A_c} \times 100$, percent
1	0.0116	0.011423	1.000	0.81	108	110	28.4×10^{-5}	----------	1.86×10^{-5}	1.360	1.86×10^{-5}	0
2	.0163	.011485	1.050	.81	116	116	59.9	----------	8.76	1.383	8.70	-0.70
3	.0340	.011370	1.525	.99	123	125	284	----------	72	1.408	71.93	-.09
4	.0575	.011310	1.530	.97	133	132	866	----------	187	1.394	186	-.54
5	.0592	.011291	1.520	.97	133	132	920	----------	436	1.413	370	-1.51
6	.0660	.011250	1.530	.96	135	137	1 182	$1\ 177\times10^{-5}$	374	1.406	420	12.30
7	.0713	.011191	1.520	.96	136	136	1 373	----------	540	1.415	539	-.18
8	.1122	.011191	1.375	.90	141	142	3 558	$3\ 588\times10^{-5}$	1070	1.411	1035	-2.03
9	.1250	.011172	1.310	.87	142	141	4 372	----------	1395	1.420	1403	.57
10	.1500	.011093	1.300	.86	142	141	6 326	$6\ 504\times10^{-5}$	1910	1.407	1961	2.68
11	.1546	.012050	1.280	.86	143	140	7 611	----------	1983	1.411	2010	1.37
12	.1805	.011072	1.260	.84	142	143	9 045	$9\ 436\times10^{-5}$	2600	1.408	2340	-10.00
13	.2060	.011003	1.240	.83	142	142	10 736	----------	2830	1.406	2815	-.53
14	.2150	.011031	1.210	.80	143	142	12 980	$13\ 386\times10^{-5}$	3060	1.422	3043	-.55
Root-mean-square value										1.410		4.30

[a]Time in position, 60 min.

TABLE III. - PARAMETERS OF LIQUID MERCURY DROPLETS IN 1.5-g ENVIRONMENT MEASURED IN 0.429-INCH INSIDE-DIAMETER GLASS TUBE

[Temperature, 82° F; relative humidity, 55 percent.]

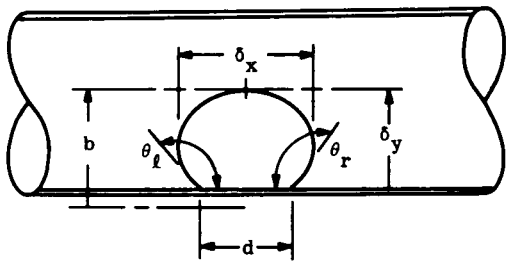

Droplet	Mean droplet diameter, δ, in.	Laplacian constant, c^2, sq in.	Size factor, $\frac{2\delta_y}{\delta}$	Shape factor, $\frac{\delta}{2b}$	Measured mean contact angle, $\theta_{s,m} = \frac{\theta_\ell + \theta_r}{2}$, deg	Calculated mean contact angle, $\theta_{s,c}$, deg	Free surface area (eq. (10)), S, sq in.	Free surface area (eq. (11)), S, sq in.	Measured tube-wall droplet contact area, A_c, sq in.	Contact area correction factor, $F = \frac{A_c}{A_{cir}}$	Contact area (eq. (23)), A, sq in.	Relative error in contact area, $\frac{A - A_c}{A_c} \times 100$, percent
1	0.0835	111.79×10^{-4}	1.54	0.95	142.0	142.5	$2\,310\times10^{-5}$	$1\,988\times10^{-5}$	693×10^{-5}	1.382	704×10^{-5}	1.59
2	.1304	111.50	1.38	.88	145.0	152.0	5 050	5 176	1615	1.377	1 614	-.06
3	.1725	111.062	1.29	.82	155.5	155.5	8 930	9 073	2520	1.398	2 526	.24
4	.1905	110.33	1.28	.80	159.0	157.5	10 930	11 161	2920	1.420	2 917	.10
5	.2380	.635	1.29	.81	159.5	158.0	17 100	17 422	3860	1.440	4 500	16.60
6	.2700	.972	1.32	.82	164.0	166.0	22 600	----------	6520	1.420	6 031	7.50
7	.3270	2.26	1.33	.83	164.0	165.5	33 100	----------	7810	1.425	7 809	-.01
8	.3635	3.43	1.31	.80	166.5	167.0	40 700	----------	8460	1.426	8 455	-.06
9	.3840	4.43	1.29	.79	167.5	169.5	46 000	----------	9986	1.434	9 978	-.60
10	.4140	5.84	1.32	.81	169.5	171.5	53 800	----------	8590	1.437	10 042	16.80
Root-mean-square value										1.42		7.50

TABLE IV. - PARAMETERS OF LIQUID MERCURY DROPLETS IN 2-g ENVIRONMENT MEASURED IN 0.429-INCH INSIDE-DIAMETER GLASS TUBE

[Temperature, 82° F; relative humidity, 55 percent.]

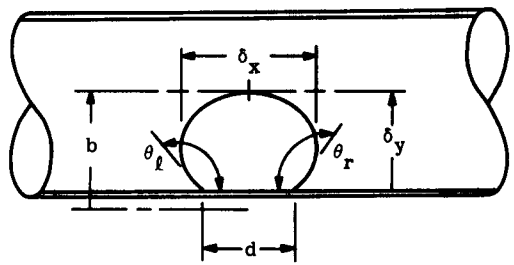

Droplet	Mean droplet diameter, δ, in.	Laplacian constant, c^2, sq in.	Size factor, $\frac{2\delta_y}{\delta}$	Shape factor, $\frac{\delta}{2b}$	Measured mean contact angle, $\theta_{s,m} = \frac{\theta_\ell + \theta_r}{2}$, deg	Calculated mean contact angle, $\theta_{s,c}$, deg	Free surface area (eq. (10)), S, sq in.	Free surface area (eq. (11)), S, sq in.	Measured tube-wall droplet contact area, A_c, sq in.	Contact area correction factor, $F = \frac{A_c}{A_{cir}}$	Contact area (eq. (24)), A, sq in.	Relative error in contact area, $\frac{A - A_c}{A_c} \times 100$, percent
1	0.0491	0.011309	1.51	0.96	137.0	134.0	642×10^{-5}	660×10^{-5}	266×10^{-5}	1.410	270×10^{-5}	1.54
2	.0677	.011255	1.41	.93	139.5	139.0	1 134	----------	543	1.680	508	-6.42
3	.0695	.011246	1.38	.90	143.0	140.5	1 234	$1\,364\times10^{-5}$	587	1.570	686	4.92
4	.0798	.011306	1.50	.94	140.5	142.0	1 651	----------	562	1.427	637	13.33
5	.0803	.011277	1.55	.94	144.0	143.5	1 796	$1\,863\times10^{-5}$	826	1.860	874	5.80
6	.0835	.011184	1.45	.91	146.0	144.0	1 873	----------	780	1.470	877	12.42
7	.1305	.011152	1.35	.88	147.0	147.5	4 880	$5\,481\times10^{-5}$	1 830	1.430	1 828	.11
8	.1673	.011073	1.27	.83	161.5	161.0	8 140	----------	2 820	1.420	2 870	1.48
9	.1822	.011066	1.28	.83	163.5	162.5	9 815	$12\,584\times10^{-5}$	3 200	1.410	3 243	1.34
10	.2240	.011000	1.28	.82	165.5	164.0	15 130	----------	4 223	1.422	4 317	2.23
11	.2250	.010930	1.30	.81	166.5	164.5	15 440	$18\,366\times10^{-5}$	4 120	1.420	4 321	2.45
Root-mean-square value										1.50		6.10

TABLE V. - PARAMETERS OF LIQUID MERCURY DROPLET MEASURED IN INCLINED 0.429-INCH INSIDE-DIAMETER GLASS TUBE

[Temperature, 80° F; relative humidity, 65 percent.]

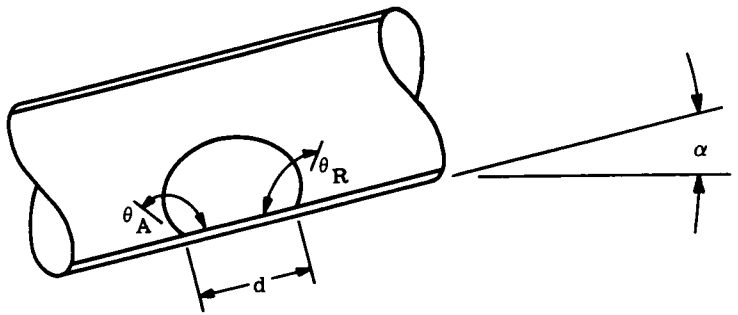

Droplet	Time-in-position, τ, min	Droplet weight, w, lb	Mean droplet diameter, δ, in.	Maximum tube inclination before droplet motion, α, deg	Calculated mean contact angle, $\theta_{s,c}$, deg	Advancing contact angle, θ_A, deg	Receding contact angle, θ_R, deg	Measured mean contact angle, $\theta_{s,m} = \frac{\theta_A + \theta_R}{2}$, deg	Distortion angle, $\Delta\theta$, deg
1	45	0.0112×10^{-3}	0.0375	29.0	125	135	115	125.0	10.0
2	60	.1340	.0875	12.0	139	148	133	140.5	7.5
3	64	.2632	.1128	8.8	141	147	136	141.5	5.5
4	67	.8150	.1875	6.2	142	148	140	144.0	4.0
5	72	.9928	.2031	5.8	144	150	144	147.0	3.0
6	80	1.2299	.2250	6.0	141	147	142	144.5	2.5
7	86	1.3783	.2374	5.6	143	144	142	143.0	1.0
8	91	1.5310	.2407	5.6	142	145	141	141.5	2.0
9	105	1.6034	.2492	5.9	143	145	141	140.5	2.0
10	120	1.6435	.2501	7.5	142	145	141	142.5	2.0

TABLE VI. - PARAMETERS OF MOVING MERCURY DROPLET IN INCLINED 0.429-INCH INSIDE-DIAMETER GLASS TUBE IN 1-g ENVIRONMENT

(a) Droplet weight, 5.288×10^{-5} ounce; droplet mean diameter in horizontal tube, 0.1283 inch; temperature, 75° F; relative humidity, 55 percent

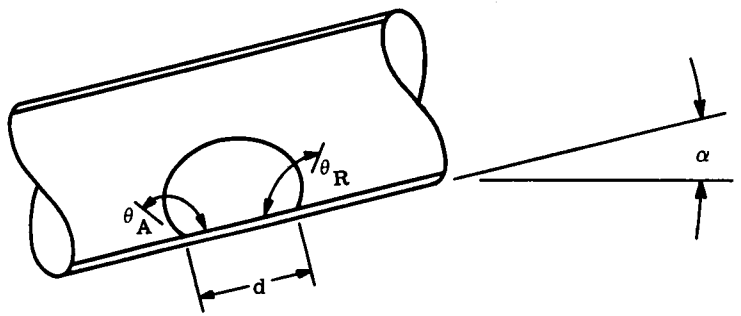

Time-in-position, τ, min	Average sliding velocity, u, in./sec	Maximum tube inclination before droplet motion, α, deg	Contact diameter of sessile droplet with solid surface, d, ft	Advancing contact angle, θ_A, deg	Receding contact angle, θ_R, deg	Mean dynamic contact angle, $\theta_d = \frac{\theta_A + \theta_R}{2}$, deg	Calculated mean contact angle, $\theta_{s,c}$, deg	Distortion angle, $\Delta\theta$, deg
10	0.064	11.00	8.044×10^{-3}	146.0	129.8	137.9	141.6	8.1
15	.152	15.42	7.883	146.8	123.8	135.3	142.4	11.5
25	.240	16.00	7.911	147.4	123.0	135.2	142.8	12.2
35	1.040	17.00	8.034	147.6	122.2	134.9	142.0	12.7
45	1.320	18.00	8.416	147.4	123.4	135.4	142.6	12.0
55	3.333	20.08	8.442	147.3	120.3	133.8	142.3	13.5

TABLE VI. - Continued. PARAMETERS OF MOVING MERCURY DROPLET IN INCLINED 0.429-INCH INSIDE-DIAMETER GLASS TUBE IN 1-g ENVIRONMENT

(b) Droplet weight, 90.736×10^{-4} ounce; droplet mean diameter in horizontal tube, 0.1541 inch; temperature, 75° F; relative humidity, 60 percent

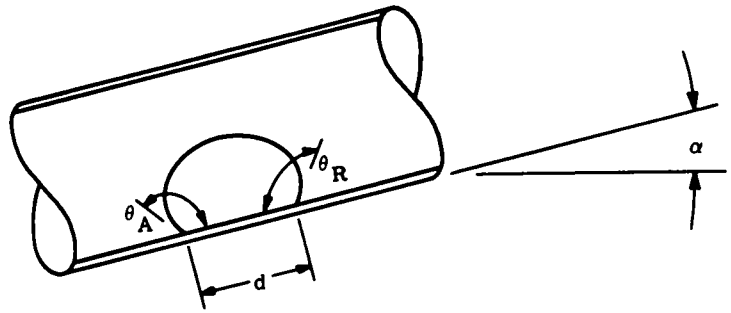

Time-in-position, τ, min	Average sliding velocity, u, in./sec	Maximum tube inclination before droplet motion, α, deg	Contact diameter of sessile droplet with solid surface, d, ft	Advancing contact angle, θ_A, deg	Receding contact angle, θ_R, deg	Mean dynamic contact angle, $\theta_d = \frac{\theta_A + \theta_R}{2}$, deg	Calculated mean contact angle, $\theta_{s,c'}$ deg	Distortion angle, $\Delta\theta$, deg
5	0.035	6.50	10.82×10^{-3}	146.3	132.6	139.4	142.3	6.8
15	.145	7.00	10.03	147.0	131.0	139.0	141.8	8.0
20	.417	8.00	10.77	147.2	130.0	138.6	140.6	8.6
25	.586	9.00	10.81	148.4	128.0	138.2	142.0	10.1
30	.900	10.00	11.31	148.7	129.2	139.0	141.6	9.2
35	2.770	12.00	11.30	149.0	125.6	137.3	142.4	11.7

TABLE VI. - Concluded. PARAMETERS OF MOVING MERCURY DROPLET IN INCLINED 0.429-INCH INSIDE-DIAMETER GLASS TUBE IN 1-g ENVIRONMENT

(c) Droplet weight, 13.664×10^{-3} ounce; droplet mean diameter in horizontal tube, 0.1953 inch; temperature, 75° F; relative humidity, 55 percent

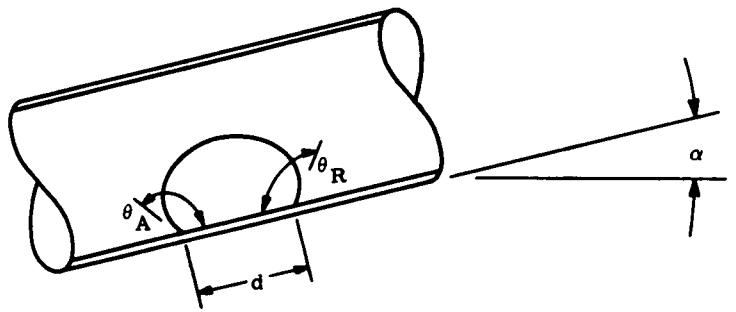

Time-in-position, τ, min	Average sliding velocity, u, in./sec	Maximum tube inclination before droplet motion, α, deg	Contact diameter of sessile droplet with solid surface, d, ft	Advancing contact angle, θ_A, deg	Receding contact angle, θ_R, deg	Mean dynamic contact angle, $\theta_d = \frac{\theta_A + \theta_R}{2}$, deg	Calculated mean contact angle, $\theta_{s,c}$, deg	Distortion angle, $\Delta\theta$, deg
5	0.064	4.50	13.37×10^{-3}	146.4	134.4	142.0	142.6	6.0
15	.145	5.00	13.08	147.5	132.4	140.0	141.7	7.6
20	.334	5.50	13.14	148.0	132.4	140.2	142.0	7.6
35	.415	6.00	13.09	148.5	131.8	140.1	143.4	8.3
45	1.000	6.50	12.86	149.0	132.1	140.6	141.5	8.5
55	1.600	7.00	13.04	149.2	131.6	140.4	140.7	8.8
65	2.860	8.00	13.37	149.0	129.8	139.4	142.8	9.5

"The aeronautical and space activities of the United States shall be conducted so as to contribute . . . to the expansion of human knowledge of phenomena in the atmosphere and space. The Administration shall provide for the widest practicable and appropriate dissemination of information concerning its activities and the results thereof."

—NATIONAL AERONAUTICS AND SPACE ACT OF 1958

NASA SCIENTIFIC AND TECHNICAL PUBLICATIONS

TECHNICAL REPORTS: Scientific and technical information considered important, complete, and a lasting contribution to existing knowledge.

TECHNICAL NOTES: Information less broad in scope but nevertheless of importance as a contribution to existing knowledge.

TECHNICAL MEMORANDUMS: Information receiving limited distribution because of preliminary data, security classification, or other reasons.

CONTRACTOR REPORTS: Technical information generated in connection with a NASA contract or grant and released under NASA auspices.

TECHNICAL TRANSLATIONS: Information published in a foreign language considered to merit NASA distribution in English.

TECHNICAL REPRINTS: Information derived from NASA activities and initially published in the form of journal articles.

SPECIAL PUBLICATIONS: Information derived from or of value to NASA activities but not necessarily reporting the results of individual NASA-programmed scientific efforts. Publications include conference proceedings, monographs, data compilations, handbooks, sourcebooks, and special bibliographies.

Details on the availability of these publications may be obtained from:

SCIENTIFIC AND TECHNICAL INFORMATION DIVISION

NATIONAL AERONAUTICS AND SPACE ADMINISTRATION

Washington, D.C. 20546